Shoot nitrate status regulates Arabidopsis shoot growth and systemic transcriptional responses via shoot adenosine phosphate-isopentenyltransferase 3

Kota Monden[a†], Takamasa Suzuki[b], Mikiko Kojima[c], Yumiko Takebayashi[c], Daisuke Sugiura[d], Tsuyoshi Nakagawa[a], Hitoshi Sakakibara[c,d], and Takushi Hachiya[a†]

[a]Department of Molecular and Functional Genomics, Interdisciplinary Center for Science Research, Shimane University, 1060 Nishikawatsu-cho, Matsue, Shimane 690-8504, Japan

[b]College of Bioscience and Biotechnology, Chubu University, 1200 Matsumoto-cho, Kasugai, Aichi 487-8501, Japan

[c]RIKEN Center for Sustainable Resource Science, 1-7-22 Suehiro-cho, Tsurumi-ku, Yokohama, Kanagawa 230-0045, Japan

[d]Graduate School of Bioagricultural Sciences, Nagoya University, Furo-cho, Chikusa-ku, Nagoya, Aichi 464-8601, Japan

[†]Corresponding authors

Corresponding authors:

Kota Monden (n23d203@matsu.shimane-u.ac.jp)

Takushi Hachiya (takushi.hachiya@life.shimane-u.ac.jp)

Funding:

This study was supported by JSPS KAKENHI [No. 20K05771 and 23K04978 to TH and No. JP24KJ1709 to KM], by JST SPRING [No. JPMJSP2155 to KM], and by the Sasakawa Scientific Research Grant from the Japan Science Society [No. 2022-4039 to KM].

Keywords:

Arabidopsis thaliana; cytokinin; IPT3; isopentenyltransferase; micrografting; NR; nitrate reductase; nitrate signal; nitrate accumulation; systemic regulation

Abstract

Plants systemically regulate growth and gene expression according to their internal nitrate status. Our previous study reported that shoot nitrate accumulation increases shoot expression of adenosine phosphate-*ISOPENTENYLTRANSFERASE 3* (*IPT3*) and shoot levels of N^6-(Δ^2-isopentenyl) adenine (iP)-type cytokinins (CKs). *IPT3* expression is localized in the phloem, and iP-type CKs, which are synthesized by IPT3, are phloem-mobile. As CKs are a class of phytohormones that control growth and genome-wide gene expression, shoot-expressed IPT3 may mediate the systemic regulation of growth and transcriptomic responses to shoot nitrate status. To examine this, we developed a novel system to manipulate nitrate levels and *IPT3* expression in a shoot-specific manner and performed growth analysis, CK determination, and RNA-sequencing. Our results demonstrated that shoot nitrate accumulation significantly promoted shoot growth and elevated shoot concentrations of iP ribotides, iP-7-*N*-glucoside, and iP-9-*N*-glucoside through the action of shoot IPT3. Transcriptomic responses to shoot nitrate accumulation were largely tuned by shoot IPT3, with opposite effects in shoots and roots. Shoot IPT3 amplified shoot responses of nitrate-inducible genes and immune response genes to shoot nitrate accumulation, while it dampened root responses of nitrate transport/assimilation genes. This transcriptomic modulation via shoot IPT3 was accompanied by coherent transcriptional changes in genes encoding mobile peptides and transcriptional repressors. Here we present a novel scheme integrating shoot nitrate status responses with CK signaling.

Introduction

Land plants use soil nitrate and ammonium as primary nitrogen sources (Hachiya and Sakakibara 2017). Root-absorbed nitrate is reduced to ammonium via the sequential actions of nitrate reductase (NR) and nitrite reductase (NiR). Ammonium, whether taken up by the roots or generated through nitrate reduction, is assimilated into Gln and Glu by the enzymes glutamine synthetase (GS) and glutamate synthase (GOGAT). These amino acids serve as precursors for the

biosynthesis of other amino acids, thereby providing carbon skeletons and amino groups for primary and secondary metabolism.

Nitrate serves as a building block for organic nitrogen biosynthesis and as a signaling molecule (Wang et al. 2004; Remans et al. 2006). The addition of exogenous nitrate to nitrate-depleted plants rapidly changes the expression of nitrate-responsive genes, a phenomenon termed ~~as~~ the primary nitrate response (PNR) (Medici and Krouk 2014). In *Arabidopsis*, the nitrate transceptor Nitrate transporter 1.1 (NRT1.1) and the transcription-activating nitrate sensor NIN-like protein 7 (NLP7) play central roles in PNR (Ho et al. 2009; Bouguyon et al. 2015; Liu et al. 2017; Liu et al. 2022). NRT1.1 physically interacts with the Cyclic nucleotide-gated channel 15 to form a nitrate-activated Ca^{2+}-permeable channel on the plasma membrane (Wang et al. 2021). Consequently, nitrate uptake via NRT1.1 transiently induces a Ca^{2+} influx, thereby elevating both cytosolic and nuclear Ca^{2+} levels (Riveras et al. 2015; Liu et al. 2017; Wang et al. 2021). Additionally, Phospholipase C also contributes to the NRT1.1-mediated increase in cytoplasmic Ca^{2+} levels (Riveras et al. 2015). The nitrate-binding affinity and uptake activity of NRT1.1 are tuned by specific protein kinases and phosphatase, including CBL-interacting protein kinases 8/23, Sucrose non-fermenting1-related protein kinase (SnRK) 2s, and ABA insensitive 2 (Ho et al. 2009; Hu et al. 2009; Léran et al. 2015; Su et al. 2020). The subgroup III Calcium-dependent protein kinases 10/30/32 (CPK10/30/32) perceive Ca^{2+} and phosphorylate NLP7 at S205, causing its nuclear retention by inhibiting nuclear export (Marchive et al. 2013; Liu et al. 2017). Nitrate-bound NLP7, along with transcription factors NLP2/6 and Nitrate regulatory gene 2—which physically interact with NLP7—promotes the transcription of PNR genes including those encoding secondary transcription factors, thereby further altering the expression of downstream targets (Konishi and Yanagisawa 2013; Xu et al. 2016; Maeda et al. 2018; Liu et al. 2022; Durand et al. 2023).

Besides its role in PNR, nitrate acts as an internal signal of plant nitrogen status, modulating nitrogen responses under steady-state conditions. In tobacco plants with different NR

activities grown under varying nitrate availability, the shoot-to-root dry weight ratio was positively correlated with foliar nitrate levels (Scheible et al. 1997). In *Arabidopsis*, abundant nitrate supply inhibits primary and lateral root growth (Zhang et al. 1998; Signora et al. 2001). Patterson et al. (2016) reported that nitrate application increases the shoot expression of glutaredoxin (Grx) genes *GrxS3/4/5/8* via Arabidopsis response regulators (ARRs) 1/10/12 for cytokinin (CK) signaling, thereby inhibiting primary root growth. Kobayashi et al. (2024) suggested that GrxS1–8 are candidate phloem-mobile signals from nitrate-supplied shoots to roots, and they bind to TGACG-binding factor 1 (TGA1) and TGA4 (Alvarez et al. 2014) in roots, forming a corepressor complex with TOPLESS to limit high-affinity nitrate uptake. Meanwhile, Ota et al. (2020) discovered that under reduced shoot nitrogen, including nitrate depletion, C-terminally encoded peptide downstream-like 2 (CEPDL2)—a Grx family protein also known as GrxS9—is induced in the leaf vasculature and subsequently translocated to the roots. The co-activator complex composed of CEPDL2, its homologs CEPD1/2, and TGA1/4 promotes root nitrate uptake (Kobayashi et al. 2024). These findings imply that shoot nitrate status influences root nitrogen acquisition.

In our previous study, to focus on the action of shoot nitrate status, we manipulated shoot nitrate levels using wild-type *Arabidopsis* and an NR-null mutant (Okamoto et al. 2019). Subsequent RNA-sequencing (RNA-seq) suggested that shoot nitrate accumulation alone represses the expression of nitrogen starvation-inducible genes in shoots and roots. Notably, we observed that shoot nitrate accumulation was accompanied by increases in the shoot expression of adenosine phosphate-*ISOPENTENYLTRANSFERASE 3* (*IPT3*) and the shoot levels of N^6-(Δ^2-isopentenyl) adenine (iP)-type CKs, including iP ribotides (iPRPs), iP-7-*N*-glucoside (iP7G), and iP-9-*N*-glucoside (iP9G) (Hachiya et al. 2020). Adenosine phosphate-IPTs including IPT3 are key enzymes that catalyze the formation of iPRPs using DMAPP as the isoprenoid donor and adenosine phosphates as acceptors (Sakakibara 2021). iP riboside 5′-monophosphate (iPRMP) is then activated to bioactive free base iP via either the one-step Lonely guy (LOG) pathway or a

105 two-step pathway involving 5′-ribonucleotide phosphohydrolase GY3 and CK/purine riboside
106 nucleosidase CPN1/NSH3 (Kurakawa et al. 2007; Kojima et al. 2023; Wu et al. 2023). iP
107 homeostasis is further fine-tuned through *N*-glucosylation catalyzed by glucosyltransferases
108 (UGTs) and degradation by cytokinin oxidase/dehydrogenases (CKXs) (Werner et al. 2003;
109 Hošek et al. 2020). CKs are a class of phytohormones that regulate a wide range of developmental
110 and physiological processes, including cell division, shoot and root growth, leaf senescence,
111 vascular formation, and responses to biotic and abiotic stresses (Werner and Schmülling 2009;
112 Cortleven et al. 2019). Multiple transcriptome analyses have demonstrated that CKs regulate
113 specific gene sets across several tissues and organs (Bhargava et al. 2013). Nitrate-induced
114 expression of *IPT3* is localized mainly in phloem cells (Miyawaki et al. 2004; Takei et al. 2004a),
115 and iP-type CKs, which are de novo synthesized by IPT3, are phloem-mobile (Hirose et al. 2008;
116 Bishopp et al. 2011). Hence, the systemic regulation of growth and transcriptomic responses to
117 shoot nitrate status may be mediated via IPT3-synthesized iP-type CKs. Supporting this idea,
118 several lines of evidence indicate both overlap and crosstalk between nitrate and CK signaling.
119 For instance, nitrate- and CK-responsive genes have been found to partially overlap (Sakakibara
120 et al. 2006). In addition, the nitrogen depletion-dependent induction of shoot *CEPDL2* is
121 enhanced by CKs translocated from roots (Ota et al. 2020). Furthermore, *trans*-zeatin (*t*Z)-type
122 CKs mediate preferential root growth in nitrate-rich patches over nitrate-poor patches (Ruffel et
123 al. 2011; Poitout et al. 2018).

124 Based on this context, the present study examined the systemic responses to shoot
125 nitrate status and their dependence on shoot IPT3. We developed a novel experimental system to
126 manipulate nitrate levels and *IPT3* expression in a shoot-specific manner using grafted plants
127 derived from plants lacking NR and/or IPT3. Using the shoots and roots of the grafted plants,
128 growth analysis, CK species determination, and RNA-seq were performed. Our results indicated
129 that shoot nitrate accumulation enhances shoot growth and alters the transcriptomes of shoots and

130 roots, which is elaborately tuned by shoot IPT3 in the opposite direction in shoots and roots. We
131 herein present a scheme incorporating shoot nitrate accumulation responses with shoot IPT3.
132
133 **Materials and Methods**
134 **Plant materials**
135 In this study, we used *A. thaliana* accession Columbia (Col) as the control line; NR-null mutant
136 (NR-null, Wang et al. 2007), *IPT3*-knockout mutant (*ipt3*, Miyawaki et al. 2006), and
137 *IPT3/IPT5/IPT7*-knockout mutant (*ipt3,5,7*, Miyawaki et al. 2006); and a transgenic plant
138 expressing *GFP* driven by the *IPT3* promoter (*proIPT3:GFP*, Takei et al. 2004a). Homozygous
139 multiple mutants of NR-null *ipt3* and NR-null *proIPT3:GFP* were produced via crossing.
140
141 **Culture media**
142 Three different solid media were used for *in vitro* plant culture as follows: (i) 2.5 mM NH_4^+
143 medium, half-strength Murashige and Skoog (1/2MS) modified basal salt mixture without
144 nitrogen (M531; PhytoTech Labs, Lenexa, KS, USA) supplemented with 1.25 mM $(NH_4)_2SO_4$,
145 10.0 g L^{-1} sucrose, 1.0 g L^{-1} MES, and 4.0 g L^{-1} gellan gum (Fujifilm Wako, Osaka, Japan) and
146 adjusted to pH 6.7 with KOH; (ii) 10 mM NO_3^- and 2.5 mM NH_4^+ medium, 1/2MS modified
147 basal salt mixture without nitrogen (M531; PhytoTech Labs) supplemented with 10 mM KNO_3,
148 1.25 mM $(NH_4)_2SO_4$, 10.0 g L^{-1} sucrose, 1.0 g L^{-1} MES, and 4.0 g L^{-1} gellan gum (Fujifilm
149 Wako) and adjusted to pH 6.7 with KOH; and (iii) no nitrogen medium, 1/2MS modified basal
150 salt mixture without nitrogen (M531; PhytoTech Labs) supplemented with 2.0 g L^{-1} sucrose, 0.5
151 g L^{-1} MES, and 5.0 g L^{-1} gellan gum (Fujifilm Wako) and adjusted to pH 5.7 with KOH. It should
152 be noted that pH 6.7 was employed to mitigate ammonium toxicity under 2.5 mM NH_4^+ medium
153 (Hachiya et al. 2021b) and to promote better growth of NR-deficient plants under 10 mM NO_3^-
154 and 2.5 mM NH_4^+ medium (Wang et al. 2004).
155

156 **Transfer experiments using grafted plants**

157 To manipulate nitrate levels and *IPT3* expression in a shoot-specific manner, micrografting and
158 transfer experiments were performed using Col, NR-null, *ipt3*, NR-null *ipt3*, and *ipt3,5,7* plants
159 (Figure 1A, B). Surface-sterilized seeds were stratified in the dark at 4°C for 3 days. To ensure
160 uniform growth regardless of the NR activity, approximately 120 seeds per dish were sown in
161 rectangular dishes (140 × 100 × 20 mm^3; Eiken Chemical Co. Ltd., Tokyo, Japan) containing 50
162 mL of 2.5 mM NH_4^+ medium and grown vertically at 22°C for 4 days under a photosynthetic
163 photon flux density (PPFD) of 25 μmol m^{-2} s^{-1} with a 16/8-h light/dark cycle (condition 1). Four-
164 day-old seedlings were grafted aseptically using four scion/rootstock combinations: Col/*ipt3,5,7*,
165 NR-null/*ipt3,5,7*, *ipt3*/*ipt3,5,7*, and NR-null *ipt3*/*ipt3,5,7* (Figure 1B). Notably, *ipt3,5,7* was used
166 as the rootstock to avoid the complementation of shoot-specific CK depletion in *ipt3* by root-
167 derived CKs. The seedlings were cut perpendicularly at the upper hypocotyl with an injection
168 needle tip (NN-2613S; TERUMO, Tokyo, Japan) on a membrane filter (HAWP04700; Merck
169 Millipore, Darmstadt, Germany). The obtained scion was connected with the partner rootstock
170 through a 0.4-mm silicone microtube (1-8194-04; AS ONE, Osaka, Japan). The grafted plants
171 were incubated at 27°C for 5 days under a PPFD of 50 μmol m^{-2} s^{-1} with a constant light
172 (condition 2) to enhance grafting success (Monden et al. 2022), and further cultivated at 22°C for
173 24 h under a PPFD of 25 μmol m^{-2} s^{-1} with a 16/8-h light/dark cycle (condition 3). Successfully
174 grafted plants without adventitious root formation were selected for size uniformity. The grafted
175 plants were transferred to round dishes (diameter, 90 mm; depth, 20 mm; AS ONE) containing 30
176 mL of 10 mM NO_3^- and 2.5 mM NH_4^+ medium and grown for 24 h under a PPFD of 25 μmol
177 m^{-2} s^{-1} with a constant light to promote nitrate accumulation in the grafted plants (condition 4).
178 Finally, the plants were transferred to round dishes containing 30 mL of no nitrogen medium and
179 grown for 5 days under a PPFD of 25 μmol m^{-2} s^{-1} with a constant light (condition 5) to allow
180 nitrate accumulation in the shoots of NR-null/*ipt3,5,7* and NR-null *ipt3*/*ipt3,5,7* but not in
181 Col/*ipt3,5,7* and *ipt3*/*ipt3,5,7*. No external nitrogen such as ammonium was supplied to avoid

182 enrichment of internal nitrogen pools and unintended signaling, which could obscure the effects
183 of shoot nitrate status. The 5-day treatment was chosen to ensure sufficient growth and
184 transcriptomic responses while minimizing transient stress caused by the pH drop from condition
185 4 to condition 5. In addition, a low light intensity of 25 μmol m^{-2} s^{-1} was employed to reduce
186 stress, given that high light intensity is known to exacerbate nitrogen deficiency stress (Iwagami
187 et al. 2022). The surfaces of no nitrogen medium were covered with cellophane sheets to allow
188 nondestructive sampling of the roots (Hachiya et al. 2021a). In conditions 2–5, four types of
189 grafted plants were grown under identical external nitrogen conditions to ensure uniform
190 biosynthesis of systemic signaling molecules responsive to external nitrogen availability, such as
191 C-terminally encoded peptides (CEPs) (Tabata et al. 2014), thereby isolating the systemic effects
192 of shoot nitrate status and enabling clearer interpretation of the results.
193
194 **Growth analysis**
195 Shoots and roots were weighed on a precision balance (HR-202i; A&D, Tokyo, Japan), and shoots
196 were scanned at a resolution of 600 dpi (GT-X980; EPSON, Tokyo, Japan) to measure the rosette
197 diameter. Leaf blades were harvested from the shoots and scanned at a resolution of 600 dpi to
198 measure the blade area of the cotyledon and true leaf. The rosette diameter and leaf blade area
199 were measured using ImageJ version 1.52p (US National Institutes of Health, Bethesda, MD,
200 USA).
201
202 **Determination of the total nitrogen content**
203 The total nitrogen concentration was quantified as previously described (Monden et al. 2022).
204 Harvested shoots and roots were oven-dried at 80°C for 2 days, and the dried samples were
205 ground using a spoon and stored in a desiccator before use. The dried powder was weighed and
206 encapsulated in a tin boat. Nitrogen concentrations were measured using a CN analyzer (Vario
207 EL III; Elementar Analysensysteme GmbH, Hanau, Germany).

208

209 **Determination of the nitrate content**

210 Nitrate content was quantified as previously described (Okamoto et al. 2019) with slight
211 modifications. Frozen samples were ground with a Multi-Beads Shocker (Yasui Kikai, Osaka,
212 Japan) using zirconia beads (diameter, 5 mm). The powder samples were boiled with 10 volumes
213 of Milli-Q water at 100°C for 20 min. Five microliters of the supernatant or 5 μL of standard
214 solution as dilution series of potassium nitrate was mixed with 40 μL of 0.05% (w/v) salicylic
215 acid in sulfuric acid. The resulting mixture was then incubated at room temperature for 20 min.
216 A mock treatment of 40 μL of sulfuric acid alone was added to 5 μL of the supernatant. One
217 microliter of 8% (w/v) NaOH solution was added to the mixture, and the nitrate content was
218 determined by measuring the absorbance at 410 nm using a plate reader (CORONA SH-9000Lab,
219 Hitachi High-Tech Corp., Tokyo, Japan).

220

221 **Observation of fluorescent signals**

222 Fluorescent imaging was performed using an All-in-one fluorescence microscope (BZ-X710,
223 KEYENCE, Osaka, Japan) with a 4× objective (CFI Plan Fluor DL 4×/0.13, Nikon, Tokyo, Japan)
224 and a metal halide lamp (No. 91056, KEYENCE). A narrow-band GFP filter (ex. 480/20; em.
225 510/20, 49020, Chroma, Brattleboro, VT, USA) and Cy5 filter (ex. 620/60; em. 700/75, 49006,
226 Chroma) were used to detect the fluorescence of GFP and chlorophyll, respectively.

227

228 **Determination of CK species**

229 The extraction and determination of CKs were performed with slight modifications to the method
230 described by Kojima et al. (2009). Frozen tissue was ground into powder using a TissueLyser
231 (Qiagen, Hilden, Germany) with a 5 mm zirconia bead. Samples were extracted in 1 ml of
232 methanol : formic acid : water (15 : 1 : 4), with stable isotope-labeled internal standards. After
233 incubation at –30°C for ≥16 h, samples were centrifuged at 10,000 × *g*, for 15 min. The

234 supernatant was collected, and the pellet was re-extracted with 0.2 ml of the same solvent.
235 Combined extracts were purified using Oasis HLB 96-well plates (Waters, Milford, MA, USA)
236 on a STAR (HAMILTON, Reno, NV, USA), followed by evaporation and reconstitution in 1 ml
237 of 1 M formic acid. Fractionation was performed on an Oasis MCX 96-well plate (Waters). ABA,
238 auxins, and gibberellins were eluted with methanol (Elution 1); CK nucleotides with 0.35 M
239 ammonia (Elution 2); and CK nucleobases, nucleosides, and glucosides with 0.35 M ammonia in
240 60% methanol (Elution 3). All fractions were dried by evaporation. For CK analysis, Elution 3
241 was reconstituted in 50 µl of 0.1% acetic acid. Elution 2 was reconstituted in 0.84 ml of 0.1 M
242 CHES-NaOH (pH 9.8), treated with 1 U μl^{-1} of alkaline phosphatase (Oriental Yeast, Tokyo,
243 Japan), incubated at 37°C for 1 h, neutralized, desalted via Oasis HLB plate, evaporated, and
244 reconstituted in 50 µl of 0.1% acetic acid. CKs were analyzed using an ultra-performance liquid
245 chromatography–tandem quadrupole mass spectrometry system (ACQUITY UPLC
246 System/XEVO-TQS; Waters) with an octadecylsilyl column (ACQUITY UPLC HSS T3, 1.8 µm,
247 2.1 mm × 100 mm; Waters). CK species were separated at a flow rate of 0.25 mL min-1 with
248 linear gradients of solvent A (0.06% acetic acid) and solvent B (0.06% acetic acid in methanol)
249 set according to the following profile: 0 min, 95% A + 5% B; 7min, 60% A + 40% B; 10 min,
250 1% A + 99% B; 10 min, 1% A + 99% B; 13 min, 95% A + 5% B.
251
252 **Determination of the total protein content**
253 The total protein content was determined as previously described (Hachiya et al. 2016). Frozen
254 samples were ground with a Multi-Beads Shocker using zirconia beads (diameter, 5 mm). Total
255 proteins were extracted with 10 vol. of Laemmli buffer (2% (w/v) SDS, 62.5 mM Tris-HCl
256 (pH 6.8), 10% (v/v) glycerol, and 0.0125% (w/v) bromophenol blue) containing Halt™ protease
257 inhibitor cocktail (Thermo Fisher Scientific, Waltman, MA, USA), followed by incubation at
258 95°C for 5 min. Extracts were centrifuged at 20,400 × *g* at room temperature for 10 min, and 10
259 µL of each aliquot was suspended in 500 µL of deionized water. Next, 100 µL of 0.15% (w/v)

260 sodium deoxycholate was added, and the mixture was incubated at room temperature for 10 min.
261 One hundred microliters of 72% (v/v) trichloroacetic acid was added, followed by incubation at
262 room temperature for 15 min and centrifugation at 20,400 × *g* for 10 min. The precipitates were
263 air-dried and suspended in 25 µL of deionized water. The suspension was analyzed with a TaKaRa
264 BCA Protein Assay Kit (T9300A, TaKaRa, Kusatsu, Japan) according to the manufacturer's
265 instructions. Protein content was determined by measuring the absorbance at 562 nm using a plate
266 reader (Hitachi High-Tech Corp.).
267
268 **RNA extraction**
269 Frozen samples were ground with a Multi-Beads Shocker using zirconia beads (diameter, 5 mm).
270 Total RNA was extracted using an RNeasy Plant Mini Kit (Qiagen) according to the
271 manufacturer's instructions. For RNA-seq library preparation, RNA was purified via on-column
272 DNase digestion (Qiagen).
273
274 **RT-qPCR and RT-sqPCR**
275 Reverse transcription (RT) was performed using a ReverTraAce qPCR RT Master Mix with
276 gDNA Remover (Toyobo, Osaka Japan). RNA solution containing 0.5 µg of template RNA
277 served as the input. Synthesized cDNA was then diluted 5-fold with water and used for
278 quantitative PCR (qPCR) and semi-quantitative PCR (sqPCR). RT-qPCR was performed on a
279 QuantStudio 1 (Thermo Fisher Scientific) with KOD SYBR qPCR Mix (Toyobo). Relative
280 transcript levels were calculated using the comparative cycle threshold method, with *ACTIN3* as
281 the internal standard (Hachiya et al. 2021b). RT-sqPCR was done on a T100 Thermal Cycler
282 (Bio-Rad Laboratories, Tokyo, Japan) with Quick Taq HS (Toyobo) under appropriate cycling
283 conditions. Primer sequences are presented in Table S1.
284
285 **RNA-seq**

286 RNA quality was evaluated using a Qubit RNA IQ Assay Kit with a Qubit 4 Fluorometer (Thermo
287 Fisher Scientific). The RNA samples for which the RNA IQs ranged 9.4–10.0 were used for RNA-
288 seq. cDNA libraries were constructed using a NEBNext Ultra II RNA Library Prep with Sample
289 Purification Beads (E7775S, New England Biolabs, Ipswich, MA, USA), a NEBNext Poly(A)
290 mRNA Magnetic Isolation Module (E7490S, New England Biolabs), and a NEBNext Multiplex
291 Oligos for Illumina (E7710S, New England Biolabs) according to the manufacturer's instructions.
292 These cDNA libraries were sequenced using NextSeq 500 (Illumina, San Diego, CA, USA), and
293 the produced bcl files were converted to fastq files using bcl2fastq (Illumina). The reads were
294 analyzed according to a previously described method (Notaguchi et al. 2014) and mapped to the
295 Arabidopsis reference (TAIR10) using Bowtie (Langmead et al. 2009) with the following options:
296 "--all --best --strata." The mapped reads were processed using iDEP version 0.96 and 2.01 (Ge et
297 al. 2018). For data normalization, the read counts data were transformed with rlog and normalized
298 by subtracting the average expression for each gene according to the default setting of iDEP. For
299 DEG extraction, DESeq2 was run with a false-discovery rate cutoff of 0.1. The enrichment
300 analysis of each gene set was conducted using Metascape (Zhou et al. 2019) according to the
301 default setting. Detailed information derived from the RNA-seq data is presented in Table S2–S9.
302

303 **Statistical analysis**

304 Unpaired two-tailed Welch's *t*-test, Tukey–Kramer multiple comparison test, two-way analysis
305 of variance (ANOVA), and hypergeometric test were performed using R software v.2.15.3 (R
306 Foundation for Statistical Computing, Vienna, Austria). The ANOVA tables are presented in
307 Table S10.
308

309 **Results and Discussion**

310 **Development of a novel system that manipulates nitrate levels and *IPT3* expression in a**
311 **shoot-specific manner**

312 To manipulate nitrate levels and *IPT3* expression in a shoot-specific manner, micrografting and
313 transfer experiments were performed using Col, NR-null, *ipt3*, NR-null *ipt3*, and *ipt3,5,7* plants
314 (Figure 1A, B). The plants were grown for 4 days in 2.5 mM NH_4^+ medium to ensure uniform
315 growth regardless of the NR activity (condition 1). Then, grafted plants corresponding to
316 Col/*ipt3,5,7*, NR-null/*ipt3,5,7*, *ipt3*/*ipt3,5,7*, and NR-null *ipt3*/*ipt3,5,7* (scion/rootstock) were
317 generated (conditions 2 and 3). Notably, *ipt3,5,7* was used as the rootstock to avoid the
318 complementation of shoot-specific CK depletion in *ipt3* by root-derived CKs. RT-sqPCR with
319 primers specific for *NIA1*, *NIA2*, *IPT3*, *IPT5*, *IPT7*, and *ACTIN2* confirmed the successful
320 generation of the desired grafted plants (Figure S1A, B). The grafted plants were transferred to
321 10 mM NO_3^- and 2.5 mM NH_4^+ medium and incubated for 24 h to allow nitrate accumulation
322 (condition 4). Then, the plants were transferred to no nitrogen medium and grown for 5 days
323 (condition 5). After nitrogen removal, nitrate concentrations generally decreased over time in the
324 shoots and roots of all plants (Figure 1C, D). At 3 and 5 days after nitrogen removal, the shoot
325 nitrate concentrations were higher in NR-null/*ipt3,5,7* and NR-null *ipt3*/*ipt3,5,7* plants than in the
326 other plants (Figure 1C), whereas root nitrate was depleted to the same level in all plants (Figure
327 1D). Meanwhile, at 5 days after nitrogen removal, total protein and total nitrogen levels in shoots
328 and roots differed little among the plants (Figure 1E–H). RT-qPCR and RNA-seq revealed that
329 shoot *IPT3* expression was significantly higher in NR-null/*ipt3,5,7* than in Col/*ipt3,5,7* (Figure 1I
330 and Figure S1C). Only minor differences in transcripts per million (TPM) of shoot *IPT1/4/5/6/7/8*
331 and root *IPT1/4/6/8* were observed among the four grafted plants (Figure S1C), suggesting that
332 adenosine phosphate-*IPT* genes other than *IPT3* did not compensate for the absence of shoot IPT3.
333 To visualize the tissue-specific induction of *IPT3* as a result of shoot NR deficiency, scions from
334 *proIPT3:GFP* and NR-null *proIPT3:GFP* plants were grafted onto *ipt3,5,7* rootstocks, followed
335 by the same transfer experiment as before. Shoot nitrate accumulation and *GFP* induction were
336 observed in NR-null *proIPT3:GFP*/*ipt3,5,7* plants 5 days after nitrogen removal (Figure 1J, K),
337 with strong GFP fluorescence localized in the leaf vein (Figure 1L). These findings suggest that

338 *IPT3* induction due to shoot nitrate accumulation occurs mainly in the vasculature. Given that
339 NLP7 promotes the *IPT3* transcription in response to nitrate application (Liu et al. 2022), it is
340 plausible that *IPT3* induction in NR-null/*ipt3,5,7* is also mediated by NLP7. Overall, we
341 successfully developed a novel system that manipulates nitrate levels and *IPT3* expression in a
342 shoot-specific manner, with minimal impact on the total protein and total nitrogen levels within
343 the plant, in the absence of external nitrogen sources. This system allows the analysis of systemic
344 responses to shoot nitrate status and their dependence on shoot IPT3 in the following experiments.
345 Furthermore, we confirmed that the TPM of nitrogen starvation-inducible *CEPs* (Tabata et al.
346 2014) did not differ significantly among the roots of grafted plants (Figure S1D). This enables us
347 to isolate the systemic effects of shoot nitrate status and shoot IPT3 independently of root-derived
348 CEP systemic signaling. All experiments described below were conducted using samples
349 collected 5 days after nitrogen removal (condition 5).
350
351 **Shoot nitrate accumulation elevates shoot levels of iP-type CKs via shoot IPT3**
352 To assess the impact of shoot nitrate status and shoot *IPT3* expression on CK activity, we
353 measured the concentrations of iP-type and *t*Z-type CKs. The experiments were performed using
354 the shoots and roots of grafted plants, with three biological replicates collected independently
355 (Figure 2) or simultaneously (Figure S2). The levels of iP, iPRPs, iP7G, iP9G, *t*Z, *t*Z ribotides
356 (*t*ZRPs), *t*Z-7-*N*-glucoside (*t*Z7G), *t*Z-9-*N*-glucoside (*t*Z9G), *t*Z-*O*-glucoside (*t*ZOG), and *t*ZR-
357 *O*-glucoside (*t*ZROG) were consistently lower in the shoots of *ipt3*/*ipt3,5,7* and NR-null
358 *ipt3*/*ipt3,5,7* plants than in those of Col/*ipt3,5,7* and NR-null/*ipt3,5,7* plants (Figure 2A, C–F, 2H–
359 L and Figure S2A, C–F, S2H–L). Meanwhile, little difference was observed in the root levels of
360 CK species among the grafted plants. These observations indicated that shoot IPT3 is crucial for
361 maintaining the shoot levels of *t*Z-type and iP-type CKs, but it has only a minor effect on root CK
362 levels. Notably, the shoot levels of iPRPs, iP7G, and iP9G were significantly increased by shoot
363 NR deficiency in the presence of shoot IPT3 but not in its absence (Figure 2C–E and Figure S2C–

364 E). This finding suggests that shoot nitrate accumulation elevates the shoot levels of these iP-type
365 CKs via shoot IPT3. However, no significant increase was observed in the levels of iP, the
366 biologically active form (Figure 2A and Figure S2A). In *Arabidopsis*, seven LOG enzymes with
367 phosphoribohydrolase activity can directly convert iPRMP into iP (Kuroha et al. 2009; Tokunaga
368 et al., 2011). Thus, elevated levels of iPRPs in the shoot likely serve as a reservoir of latent CK
369 activity, with the potential to regulate growth and gene expression depending on the spatial and
370 temporal activity of LOG enzymes. Given that Arabidopsis *LOG* genes exhibit distinct spatial
371 expression patterns (Kuroha et al. 2009), the iPRPs accumulated in response to shoot nitrate
372 accumulation may be locally converted to iP in cells or tissues expressing specific LOG isoforms.
373 While our CK quantifications were performed using whole shoots and roots, it is possible that
374 localized changes in iP concentrations —for example, in actively growing regions such as the
375 shoot apical meristem or the basal zone of young leaves—were not captured. Targeted sampling
376 of these regions may therefore be necessary to reveal the spatial dynamics of iP production in
377 response to shoot nitrate status.
378
379 **Shoot nitrate accumulation enhances shoot growth via shoot IPT3**
380 To determine the effects of shoot nitrate status and shoot *IPT3* expression on plant growth, we
381 analyzed growth parameters using all grafted plants from five independent experiments (Figure
382 3). Shoot fresh weight, leaf blade area, rosette diameter, and leaf number were significantly lower
383 in *ipt3*/*ipt3,5,7* and NR-null *ipt3*/*ipt3,5,7* plants than in Col/*ipt3,5,7* and NR-null/*ipt3,5,7* plants
384 (Figure 3B–E). Meanwhile, no significant difference was observed in the root fresh weight among
385 the grafted plants (Figure 3F). These observations indicate that shoot IPT3 generally contributes
386 to shoot growth. Importantly, shoot appearance, shoot fresh weight, and leaf blade area were
387 significantly increased by shoot NR deficiency in the presence of shoot IPT3 but not in its absence
388 (Figure 3A–C). A similar trend was observed for the rosette diameter, although the differences
389 were not statistically significant (Figure 3D). These patterns correspond to the findings for shoot

iPRPs, iP7G, and iP9G concentrations (Figure 2C–E and Figure S2C–E). Actually, shoot fresh weight and leaf blade area were strongly correlated with levels of these iP-type CKs (Figure S3). In *Arabidopsis*, iPRPs and the glucosides iP7G and iP9G are generally considered biologically inactive CKs (Tokunaga et al. 2011; Hoyerová and Hošek 2020) and thus unlikely to directly promote shoot growth. Among iPRPs, iPRMP can be rapidly converted into bioactive iP by LOG enzymes, thereby activating CK signaling (Kurakawa et al. 2007; Kuroha et al. 2009). By contrast, iP7G and iP9G are not converted into other CKs (Hošek et al. 2020), precluding their contribution to shoot growth. Nevertheless, because bioactive iP is predominantly metabolized to iP7G (Hošek et al., 2020) and iP7G resists degradation by Arabidopsis CKXs (Galuszka et al., 2007), iP7G may serve as a proxy for iP-dependent signaling. Overall, our findings suggest that shoot nitrate accumulation promotes shoot growth by increasing IPT3 and iP-type CK biosynthesis in the shoot. It is well established that in Arabidopsis plants, root-supplied nitrate stimulates the biosynthesis of *t*Z-type CKs in the root and facilitates their transport to the shoot, thereby promoting shoot growth (Kiba et al. 2013; Ko et al. 2014; Osugi et al. 2017; Sakakibara, 2021). Collectively, shoot-derived iP-type CKs and root-derived *t*Z-type CKs may regulate shoot growth by responding to the internal and external nitrate status, respectively. Interestingly, the fresh weight ratios of shoot to root were significantly elevated by shoot NR deficiency in the presence of shoot IPT3 but not in its absence (Figure 3G). Given that, in general, biomass ratios of shoot to root are positively correlated with overall nitrogen availability both inside and outside the plant (Andrews et al. 2006; Krapp et al. 2011; Hachiya et al. 2014), our findings support the idea that shoot nitrate status serves as an indicator of nitrogen availability. Furthermore, since CK action is known to enhance sink activity (Werner et al. 2008), it is plausible that shoot nitrate status influences shoot CK levels and subsequently biomass allocation ~~between shoot and root~~ via shoot IPT3-mediated CK signaling.

415 **Shoot IPT3 oppositely modulates transcriptomic responses to shoot nitrate accumulation in**
416 **shoots and roots**
417 To investigate the effects of shoot nitrate status and shoot *IPT3* expression on systemic responses,
418 we performed RNA-seq using the shoots and roots of grafted plants, with three biological
419 replicates collected independently. Reads per million mapped reads (RPM; Table S2) and
420 normalized transcript levels (Table S3) were calculated according to the read counts. To identify
421 genes regulated by shoot nitrate accumulation and further modulated by shoot IPT3, we extracted
422 differentially expressed genes (DEGs) between NR-null/*ipt3,5,7* and Col/*ipt3,5,7* and between
423 NR-null *ipt3*/*ipt3,5,7* and *ipt3*/*ipt3,5,7* with a minimum fold change of 1.5 (Figure 4A and Figure
424 S4 and Table S4). Comparison of these DEGs between shoots and roots revealed minimal overlap
425 (Figure S4), indicating that shoots and roots express distinct sets of genes regulated by shoot
426 nitrate accumulation. Hence, we analyzed the shoot and root transcriptomes separately. Notably,
427 in shoots, the number of DEGs was larger between NR-null/*ipt3,5,7* and Col/*ipt3,5,7* than
428 between NR-null *ipt3*/*ipt3,5,7* and *ipt3*/*ipt3,5,7* (Figure 4A). By contrast, in roots, the number of
429 DEGs was lower between NR-null/*ipt3,5,7* and Col/*ipt3,5,7* than between NR-null *ipt3*/*ipt3,5,7*
430 and *ipt3*/*ipt3,5,7* (Figure 4A). These observations suggest that shoot transcriptional responses to
431 shoot nitrate accumulation are enhanced by shoot IPT3, whereas root responses are attenuated by
432 shoot IPT3. To substantiate this, we quantitatively analyzed the 631 and 663 DEGs identified
433 exclusively between NR-null/*ipt3,5,7* and Col/*ipt3,5,7* in shoots, and the 189 and 126 DEGs
434 identified exclusively between NR-null *ipt3*/*ipt3,5,7* and *ipt3*/*ipt3,5,7* in roots (Figure 4A). The
435 shoot transcriptional responses of 631 upregulated and 663 downregulated DEGs to shoot NR
436 deficiency were decreased by shoot IPT3 deficiency (Figure 4B, C). Conversely, the root
437 responses of 189 upregulated and 126 downregulated DEGs were augmented by shoot IPT3
438 deficiency (Figure 4D, E). Furthermore, k-means clustering identified 11 out of 16 clusters
439 (clusters 1–3, 6–8, 11, 12, and 14–16) in which gene expression was significantly altered by shoot
440 NR deficiency, with their responses decreased by shoot IPT3 deficiency in shoots but increased

441 in roots (Figure S5, S6 and Table S5). In summary, we conclude that shoot transcriptional
442 responses to shoot nitrate accumulation are generally enhanced by shoot IPT3, whereas root
443 responses are dampened by shoot IPT3. It should be noted that three independent RNA-seq results
444 exhibited similar trends; therefore, only the mean transcript levels are presented in subsequent
445 figures for clarity, unless otherwise stated.

446 Enrichment analyses of the 11 clusters from Figure S5 and S6 revealed a diverse set
447 of genes significantly regulated by shoot nitrate and shoot IPT3. In shoots, the cluster 6 and 8
448 enriched terms related to translation, primary carbon metabolism, and biotic stress response such
449 as "ath03010: Ribosome", "WP2621: Glycolysis", and "GO:0009617: response to bacterium"
450 (Figure S5A). Previously, we reported that shoot nitrate accumulation is accompanied by the
451 upregulation of ribosome-associated genes in shoots (Hachiya et al. 2020). It is widely known
452 that CK signal upregulates genes encoding ribosomal proteins and elongation factors (Sakakibara
453 et al. 2006). Hence, translation may be activated by shoot nitrate accumulation, some of which
454 are mediated by shoot IPT3 (Figure S5B). Meanwhile, terms related to wounding and jasmonic
455 acids were overrepresented in both cluster 3 and 7 (Figure S5A). Thus, stress responses associated
456 with jasmonic acids signaling could be downregulated by shoot nitrate accumulation, which is
457 enhanced by shoot IPT3 (Figure S5B). In roots, the cluster 11, 12, and 14 predominantly featured
458 terms related to abiotic and biotic stresses, particularly hypoxia (Figure S6A). The cluster 15 and
459 16 enriched terms associated with translation, biosynthesis, and nitrate transport (Figure S6A).
460 Notably, the genes encoding high-affinity nitrate transporters (*NRT2.1*, *NRT2.4*, *NRT2.5*, *NRT3.1*)
461 and nitrate reductases (*NIA1*, *NIA2*) were included in the cluster 16 (Table S5). Thus, shoot nitrate
462 accumulation may suppress nitrate uptake and assimilation in the roots, the responses of which
463 are dampened by shoot IPT3 (Figure S6B).

464

465 **Shoot nitrate accumulation induces shoot *ARR2* expression via shoot IPT3**

466 To investigate CK responses associated with altered shoot iP-type CKs and shoot growth, we first
467 examined the shoot expression of representative CK-inducible genes using a reference list
468 compiled from multiple studies (Bhargava et al. 2013). However, their expression showed
469 statistically significant but slight decreases due to shoot IPT3 deficiency, whereas no significant
470 changes were detected with shoot NR deficiency (Figure S7A and Table S6). Notably, previous
471 studies analyzed early transcriptomic responses to exogenous application of *t*Z and benzyladenine
472 (Bhargava et al. 2013); therefore, conventional gene lists might be unsuitable for evaluating
473 steady-state responses to alterations of endogenous iP-type CKs. Next, to further dissect CK-
474 related components, we focused on CK signaling- and metabolism-related genes, including those
475 encoding ARRs, cytokinin response factors (CRFs), cytochrome P450 monooxygenases
476 (CYP735A1/A2), UGTs, and CKXs (Werner et al. 2003; Rashotte and Goertzen 2010; Kiba et al.
477 2013; Hošek et al. 2020) (Figure S7B). Among these, shoot expression of the type-B *ARR2* was
478 induced by shoot NR deficiency in the presence of shoot IPT3 but not in its absence (Figure S7B),
479 a finding corroborated by RT-qPCR (Figure S7C). Choi et al. (2010) demonstrated that CK-
480 activated ARR2 enhances Arabidopsis immunity through direct binding with the transcription
481 factor TGA3. In Figure S5A, the cluster 8 derived from clustering was overrepresented in terms
482 such as "GO:0009617: response to bacterium" and "GO:0009627: systemic acquired resistance"
483 (Figure S5A). Thus, shoot nitrate accumulation might enhance immunity by upregulating *ARR2*
484 via shoot IPT3. Furthermore, given that *ARR2*-overexpressing plants exhibit larger rosette leaves
485 and biomass (Arnaud et al. 2017), it is plausible that shoot nitrate accumulation could promote
486 shoot growth partly via shoot IPT3–ARR2 module.
487
488 **Shoot IPT3 enhances transcriptional responses of nitrate–CPKs–NLPs-regulatory genes to**
489 **shoot nitrate accumulation**
490 Previously, we reported that the expression of nitrate-responsive genes is influenced by shoot
491 nitrate accumulation (Okamoto et al. 2019), prompting our focus on these genes. In shoots, the

492 transcript levels of genes induced by nitrate itself (Wang et al. 2004) were significantly increased
493 by shoot NR deficiency, and this induction was attenuated by shoot IPT3 deficiency (Figure 5A
494 and Table S7). By contrast, there was minimal variation in the root expression of nitrate-inducible
495 genes among the plants. Given that CPK10/30/32, NLP7, and its homologs (NLPs) govern nitrate-
496 dependent gene expression (Liu et al. 2017; Liu et al. 2022), we analyzed the expression of genes
497 induced by the nitrate–CPKs–NLPs signaling pathway. In shoots, the genes induced via
498 CPK10/30/32 and those co-induced via all NLPs exhibited similar expression patterns as the
499 nitrate-inducible genes (Figure 5A–C and Table S7). Meanwhile, none of the genes induced
500 exclusively by individual NLPs exhibited different expression patterns among the plants (Figure
501 S8 and Table S8). In roots, the expression of genes regulated via CPK10/30/32 and NLPs showed
502 little variation among the plants (Figure 5B, C and Figure S8 and Table S7, S8). These findings
503 suggest that shoot nitrate accumulation upregulates nitrate-inducible genes via CPK10/30/32 and
504 multiple NLPs specifically in the shoots, with their responses enhanced by shoot IPT3.
505
506 **Shoot IPT3 oppositely modulates transcriptional responses of nitrogen starvation-inducible**
507 **genes to shoot nitrate accumulation in shoots and roots**
508 Previously, we reported that shoot nitrate accumulation alleviates nitrogen starvation responses
509 (Okamoto et al. 2019). Thus, we analyzed the responses of two independent sets of nitrogen
510 starvation-inducible gene (Krapp et al. 2011; Kiba et al. 2018) (Table S9). Although these gene
511 sets are quite distinct (Figure S9A), shoot NR deficiency consistently repressed shoot expression
512 of nitrogen starvation-inducible genes, with this repression slightly alleviated by shoot IPT3
513 deficiency (Figure S9B, C). The nitrogen starvation-inducible genes common to both gene sets
514 exhibited a similar but stronger tendency (Figure 5D). Meanwhile, the root expression of nitrogen
515 starvation inducible-genes were significantly repressed by shoot NR deficiency only in the
516 absence of shoot IPT3 (Figure 5D and S9B, C). Overall, upon nitrate accumulation in shoots,

517 shoot IPT3 enhances the repression of nitrogen starvation-inducible genes in shoots but attenuates
518 this repression in roots.

519 Several genes involved in nitrogen transport and assimilation in the root are often
520 induced under nitrogen starvation (Krapp et al. 2011; Kiba et al. 2018), and thus, we focused on
521 their root expression. Most of the genes involved in high-affinity nitrate uptake and nitrogen
522 assimilation were slightly downregulated by shoot NR deficiency, and these responses were
523 remarkably intensified by shoot IPT3 deficiency (Figure 5E). Thus, the degree of downregulation
524 in root nitrate utilization due to shoot nitrate accumulation is largely dependent on shoot IPT3.
525 By contrast, genes involved in dual-affinity/low-affinity nitrate transport (*NRT1.1* and *NRT1.2*)
526 (Liu et al. 1999) were upregulated by shoot NR deficiency regardless of the presence of shoot
527 IPT3 (Figure 5E). Because NRT1.1 and NRT1.2 can facilitate the uptake of auxin and abscisic
528 acid, respectively (Krouk et al. 2010; Kanno et al. 2012), their upregulation may not necessarily
529 be related to nitrate acquisition.

530

531 **Systemic regulation of nitrogen starvation-inducible genes by shoot nitrate accumulation**
532 **may involve transcriptional repressors and mobile peptides**

533 Nitrate signaling induces the expression of genes encoding Nitrate-inducible GARP-type
534 transcriptional repressor 1 family proteins (NIGT1.1/1.2/1.3/1.4) and LOB domain-containing
535 proteins 37/38/39 (LBD37/38/39) via NLPs (Rubin et al. 2009; Marchive et al. 2013; Kiba et al.
536 2018; Maeda et al. 2018; Safi et al 2021). These proteins act as repressors of nitrogen starvation-
537 inducible genes; therefore, we examined their encoding genes. In the shoot, the transcript levels
538 of *NIGT1.1* and *LBD37/38* were increased by shoot NR deficiency, and this induction was
539 attenuated by shoot IPT3 deficiency (Figure 5F and S10A). The expression of these repressors
540 exhibited a strong negative correlation with that of nitrogen starvation-inducible genes in the
541 shoot (Figure S10B). In the root, the transcript levels of *NIGT1.1/1.2* and *LBD37/38* were
542 increased by shoot NR deficiency, and this induction was enhanced by shoot IPT3 deficiency

543 (Figure 5G and S10C). Interestingly, root *LBD39* expression was induced by shoot NR deficiency
544 only in the absence of shoot IPT3. These repressors also showed a strong negative correlation
545 with nitrogen starvation-inducible genes in the root (Figure S10D). These findings suggest that
546 shoot nitrate accumulation and shoot IPT3 regulate the systemic regulation of nitrogen starvation-
547 inducible genes via these repressors. It is valuable to explore whether iP-type CKs synthesized
548 by shoot IPT3 systemically regulate the root expression of repressor genes.

549 Next, we focused on candidate shoot-to-root mobile peptides regulating systemic
550 nitrogen responses, i.e., CEPD1/2, CEPDL2, and GrxS1–8 (Ohkubo et al. 2017; Ota et al. 2020;
551 Kobayashi et al. 2024) (Figure 5H and S11). The co-activator complexes composed of
552 CEPD1/2/CEPDL2 and TGA1/4 promote root nitrate uptake via upregulation of *NRT2.1* and
553 *CEPH*, whereas the co-repressor complexes of GrxS1–8 and TGA1/4 repress it (Kobayashi et al.
554 2024). In the shoot, *CEPDL2* transcript levels were reduced by shoot NR deficiency, and this
555 repression was attenuated by shoot IPT3 deficiency (Figure 5H and S11A). In contrast, shoot
556 *GrxS3* expression was upregulated by shoot NR deficiency, and this induction was slightly
557 enhanced in the absence of shoot IPT3. Interestingly, shoot *GrxS5* expression was induced by
558 shoot NR deficiency only in the absence of shoot IPT3. The root expression of *NRT2.1* and *CEPH*
559 was positively correlated with shoot expression of *CEPDL2*, whereas negatively correlated with
560 shoot expression of *GrxS3* and *GrxS5* (Figure S11B). These findings suggest that shoot nitrate
561 status and shoot IPT3 regulate root high-affinity nitrate uptake via shoot-to-root mobile peptides.
562

563 **Conclusion: a scheme integrating shoot nitrate accumulation responses with shoot IPT3**

564 Our experimental system elucidated the systemic responses to shoot nitrate status and their
565 dependence on shoot IPT3. A novel scheme for the systemic responses is summarized in Figure
566 6: shoot nitrate accumulation promotes shoot growth and induces the shoot expression of *IPT3*,
567 nitrate–CPKs–NLPs-inducible genes (including those for nitrate uptake/assimilation), and
568 immune response genes, with their responses enhanced by shoot IPT3. Meanwhile, shoot nitrate

accumulation decreases the root expression of nitrogen starvation-inducible genes and nitrate uptake/assimilation genes, with their responses dampened by shoot IPT3. These interactive effects of shoot nitrate status and shoot IPT3 were confirmed by two-way ANOVA, which detected statistically significant interactions between the presence or absence of shoot NR and shoot IPT3 (Table S10). Hence, under shoot nitrate accumulation, shoot IPT3 would promote nitrogen utilization at the whole-plant scale, providing organic nitrogen crucial for shoot growth enhancement. Notably, plant CK levels are generally reduced by prolonged abiotic stresses including salinity, drought, chilling, and heat (Cortleven et al. 2019), during which shoot growth is usually suppressed. Thus, shoot growth and nitrogen utilization, which are tuned by shoot IPT3 depending on shoot nitrate status, would be further fine-tuned via modulation of CK levels depending on abiotic stresses. Such crosstalk in CK signaling would optimize plant growth and nitrogen utilization in fluctuating environments. Despite these insights, it remains challenging to distinguish between primary and secondary responses to shoot nitrate accumulation, as well as to evaluate the potential effects of organic nitrogen compounds such as Gln, a candidate nitrogen status signal (Nacry et al., 2013), which were not quantified in this study. In addition, it is unclear exactly where and how the phloem-mobile iP-type CKs produced by shoot IPT3 trigger downstream signaling to orchestrate systemic responses. Furthermore, the cell types, subcellular compartments, and molecular mechanisms involved in sensing shoot nitrate status are entirely unknown. Future studies should address these unresolved questions.

Author contributions

TH: conceptualization; TS: data curation; KM and TH: formal analysis; KM and TH: funding acquisition; KM, TS, MK, YT, and DS: investigation; KM: methodology; KM and TH: project administration; KM and TH: resources; TN, HS, and TH: supervision; KM and TH: validation; KM and TH: visualization; TH: writing – original draft preparation; All authors: writing – review & editing.

Acknowledgements

The NR-null seeds were kindly provided by Dr. Nigel M. Crawford (University of California, San Diego). The *ipt3* and *ipt3,5,7* seeds were kindly provided by Dr. Tatsuo Kakimoto (Osaka University). We thank Ms. Yuki Okamoto and Mr. Masahiro Watanabe for their support in the preparation of the plant materials. This study was supported by JSPS KAKENHI [No. 20K05771 and 23K04978 to TH and No. JP24KJ1709 to KM], by JST SPRING [No. JPMJSP2155 to KM], and by the Sasakawa Scientific Research Grant from the Japan Science Society [No. 2022-4039 to KM].

Conflicts of interest

The authors declare no competing interests.

Data Availability Statement

The RNA-seq raw data are available in ArrayExpress under the accession number E-MTAB-14302 (https://www.ebi.ac.uk/biostudies/arrayexpress).

References

Alvarez, J. M., E. Riveras, E. A. Vidal, et al. 2014. "Systems approach identifies TGA1 and TGA4 transcription factors as important regulatory components of the nitrate response of *Arabidopsis thaliana* roots." *Plant Journal* 80 : 1–13. https://doi.org/10.1111/tpj.12618.

Andrews, M., J. A. Raven, P. J. Lea, and J. I. Sprent. 2006. "A role for shoot protein in shoot–root dry matter allocation in higher plants." *Annals of Botany* 97: 3–10. https://doi.org/10.1093/aob/mcj009.

621 Arnaud, D., S. Lee, Y. Takebayashi, et al. 2017. "Cytokinin-mediated regulation of reactive
622 oxygen species homeostasis modulates stomatal immunity in Arabidopsis." *Plant Cell* 29: 543–
623 559. https://doi.org/10.1105/tpc.16.00583.
624
625 Bhargava, A., I. Clabaugh, J. P. To, et al. 2013. "Identification of cytokinin-responsive genes
626 using microarray meta-analysis and RNA-Seq in Arabidopsis." *Plant Physiology* 162: 272–294.
627 https://doi.org/10.1104/pp.113.217026.
628
629 Bishopp, A., S. Lehesranta, A. Vatén, et al. 2011. "Phloem-transported cytokinin regulates polar
630 auxin transport and maintains vascular pattern in the root meristem." *Current Biology* 21: 927–
631 932. https://doi.org/10.1016/j.cub.2011.04.049.
632
633 Bouguyon, E., F. Brun, D. Meynard, et al. 2015. "Multiple mechanisms of nitrate sensing by
634 *Arabidopsis* nitrate transceptor NRT1.1." *Nature Plants* 1: 15015.
635 https://doi.org/10.1038/nplants.2015.15.
636
637 Choi, J., S. U. Huh, M. Kojima, H. Sakakibara, K. H. Paek, and I. Hwang. 2010. "The cytokinin-
638 activated transcription factor ARR2 promotes plant immunity via TGA3/NPR1-dependent
639 salicylic acid signaling in *Arabidopsis*." *Developmental Cell* 19: 284–295.
640 https://doi.org/10.1016/j.devcel.2010.07.011.
641
642 Cortleven, A., J. E. Leuendorf, M. Frank, D. Pezzetta, S. Bolt, and T. Schmülling. 2019.
643 "Cytokinin action in response to abiotic and biotic stresses in plants." *Plant, Cell & Environment*
644 42: 998–1018. https://doi.org/10.1111/pce.13494.
645

646 Durand, M., V. Brehaut, G. Clement, et al. 2023. "The Arabidopsis transcription factor NLP2
647 regulates early nitrate responses and integrates nitrate assimilation with energy and carbon
648 skeleton supply." *Plant Cell* 35: 1429–1454. https://doi.org/10.1093/plcell/koad025.
649
650 Galuszka P., H. Popelková, T. Werner, et al. 2007. "Biochemical characterization of cytokinin
651 oxidases/dehydrogenases from *Arabidopsis thaliana* expressed in *Nicotiana tabacum* L." *Journal*
652 *of Plant Growth Regulation* 26: 255–267.
653
654 Ge, S. X., E. W. Son, and R. Yao. 2018. "iDEP: an integrated web application for differential
655 expression and pathway analysis of RNA-Seq data." *BMC Bioinformatics* 19: 534.
656 https://doi.org/10.1186/s12859-018-2486-6.
657
658 Hachiya, T., D. Sugiura, M. Kojima, et al. 2014. "High CO_2 triggers preferential root growth of
659 *Arabidopsis thaliana* via two distinct systems under low pH and low N stresses." *Plant & Cell*
660 *Physiology* 55: 269–280. https://doi.org/10.1093/pcp/pcu001.
661
662 Hachiya, T., N. Ueda, M. Kitagawa, et al. 2016. "Arabidopsis root-type ferredoxin:NADP(H)
663 oxidoreductase 2 is involved in detoxification of nitrite in roots." *Plant & Cell Physiology* 57:
664 2440–2450. https://doi.org/10.1093/pcp/pcw158.
665
666 Hachiya, T., and H. Sakakibara. 2017. "Interactions between nitrate and ammonium in their
667 uptake, allocation, assimilation, and signaling in plants." *Journal of Experimental Botany* 68:
668 2501-2512. https://doi.org/10.1093/jxb/erw449.
669

670 Hachiya, T., Y. Okamoto, M. Watanabe, et al. 2020. "Genome-wide responses to shoot nitrate
671 satiety are attenuated by external ammonium in *Arabidopsis thaliana*." *Soil Science and Plant*
672 *Nutrition* 66: 317–327. https://doi.org/10.1080/00380768.2020.1717905.
673
674 Hachiya, T., T. Oya, K. Monden, A. Nagae, and T. Nakagawa. 2021a. "A cellophane-supported
675 *Arabidopsis* culture for seamless transfer between different media is useful for studying various
676 nitrogen responses." *Soil Science and Plant Nutrition* 67: 277–282.
677 https://doi.org/10.1080/00380768.2021.1908094.
678
679 Hachiya, T., J. Inaba, M. Wakazaki, et al. 2021b. "Excessive ammonium assimilation by plastidic
680 glutamine synthetase causes ammonium toxicity in *Arabidopsis thaliana*." *Nature*
681 *Communications* 12: 4944. https://doi.org/10.1038/s41467-021-25238-7.
682
683 Hirose, N., K. Takei, T. Kuroha, T. Kamada-Nobusada, H. Hayashi, and H. Sakakibara. 2008.
684 "Regulation of cytokinin biosynthesis, compartmentalization and translocation." *Journal of*
685 *Experimental Botany* 59: 75–83. https://doi.org/10.1093/jxb/erm157.
686
687 Ho, C. H., S. H. Lin, H. C. Hu, and Y. F. Tsay. 2009. "CHL1 functions as a nitrate sensor in
688 plants." *Cell* 138: 1184–1194. https://doi.org/10.1016/j.cell.2009.07.004.
689
690 Hošek P., K. Hoyerová, N. S. Kiran, et al. 2020. "Distinct metabolism of *N*-glucosides of
691 isopentenyladenine and *trans*-zeatin determines cytokinin metabolic spectrum in Arabidopsis."
692 *New Phytologist* 225: 2423–2438. https://doi.org/10.1111/nph.16310.
693
694 Hoyerová, K., P. Hošek. 2020. "New insights into the metabolism and role of cytokinin *N*-
695 glucosides in plants." *Frontiers in Plant Science* 11: 741. https://doi.org/10.3389/fpls.2020.00741.

Hu, H. C., Y. Y. Wang, and Y. F. Tsay. 2009. "AtCIPK8, a CBL-interacting protein kinase, regulates the low-affinity phase of the primary nitrate response." *Plant Journal* 57: 264–278. https://doi.org/10.1111/j.1365-313X.2008.03685.x.

Iwagami, T., T. Ogawa, T. Ishikawa, and T. Maruta. 2022. "Activation of ascorbate metabolism by nitrogen starvation and its physiological impacts in *Arabidopsis thaliana*." *Bioscience, Biotechnology, and Biochemistry* 86: 476–489. https://doi.org/10.1093/bbb/zbac010.

Kanno, Y., A. Hanada, Y. Chiba, et al. 2012. "Identification of an abscisic acid transporter by functional screening using the receptor complex as a sensor." *Proceedings of the National Academy of Sciences of the United States of America* 109: 9653–9658. https://doi.org/10.1073/pnas.1203567109.

Kiba, T., K. Takei, M. Kojima, and H. Sakakibara. 2013. "Side-chain modification of cytokinins controls shoot growth in *Arabidopsis*." *Developmental Cell* 27: 452–461. https://doi.org/10.1016/j.devcel.2013.10.004.

Kiba, T., J. Inaba, T. Kudo, et al. 2018. "Repression of nitrogen starvation responses by members of the Arabidopsis GARP-type transcription factor NIGT1/HRS1 subfamily." *Plant Cell* 30: 925–945. https://doi.org/10.1105/tpc.17.00810.

Ko, D., J. Kang, T. Kiba, et al. 2014. "*Arabidopsis* ABCG14 is essential for the root-to-shoot translocation of cytokinin." *Proceedings of the National Academy of Sciences of the United States of America* 111: 7150–7155. https://doi.org/10.1073/pnas.1321519111.

722 Kobayashi, R., Y. Ohkubo, M. Izumi, et al. 2024. "Integration of shoot-derived polypeptide
723 signals by root TGA transcription factors is essential for survival under fluctuating nitrogen
724 environments." *Nature Communications* 15: 6903. https://doi.org/10.1038/s41467-024-51091-5.
725
726 Kojima, M., T. Kamada-Nobusada, H. Komatsu, et al. 2009. "Highly sensitive and high-
727 throughput analysis of plant hormones using MS-probe modification and liquid chromatography–
728 tandem mass spectrometry: an application for hormone profiling in *Oryza sativa*." *Plant & Cell*
729 *Physiology* 50: 1201–1214. https://doi.org/10.1093/pcp/pcp057.
730
731 Kojima, M., N. Makita, K. Miyata, et al. 2023. "A cell wall–localized cytokinin/purine riboside
732 nucleosidase is involved in apoplastic cytokinin metabolism in *Oryza sativa*." *Proceedings of the*
733 *National Academy of Sciences of the United States of America* 120: e2217708120.
734 https://doi.org/10.1073/pnas.221770812.
735
736 Konishi, M., and S. Yanagisawa. 2013. "Arabidopsis NIN-like transcription factors have a central
737 role in nitrate signalling." *Nature communications* 4: 1617. https://doi.org/10.1038/ncomms2621.
738
739 Krapp, A., R. Berthomé, M. Orsel, et al. 2011. "Arabidopsis roots and shoots show distinct
740 temporal adaptation patterns toward nitrogen starvation." *Plant Physiology* 157: 1255–1282.
741 https://doi.org/10.1104/pp.111.179838.
742
743 Krouk, G, B. Lacombe, A. Bielach, et al. 2010. "Nitrate-regulated auxin transport by NRT1.1
744 defines a mechanism for nutrient sensing in plants." *Developmental Cell* 18: 927–937.
745 https://doi.org/10.1016/j.devcel.2010.05.008.
746

Kurakawa T., N. Ueda, M. Maekawa, et al. 2007. “Direct control of shoot meristem activity by a cytokinin-activating enzyme.” *Nature* 445: 652–655. https://doi.org/10.1038/nature05504.

Kuroha, T., H. Tokunaga, M. Kojima, et al. 2009. “Functional analyses of *LONELY GUY* cytokinin-activating enzymes reveal the importance of the direct activation pathway in *Arabidopsis*.” *Plant Cell* 21: 3152–3169. https://doi.org/10.1105/tpc.109.068676.

Langmead, B., C. Trapnell, M. Pop, and S. L. Salzberg. 2009. “Ultrafast and memory-efficient alignment of short DNA sequences to the human genome.” *Genome Biology* 10: R25. https://doi.org/10.1186/gb-2009-10-3-r25.

Léran, S., K. H. Edel, M. Pervent, et al. 2015. “Nitrate sensing and uptake in *Arabidopsis* are enhanced by ABI2, a phosphatase inactivated by the stress hormone abscisic acid.” *Science Signaling* 8: ra43. DOI: 10.1126/scisignal.aaa4829.

Liu, K. H., C. Y. Huang, and Y. F. Tsay. 1999. “CHL1 is a dual-affinity nitrate transporter of Arabidopsis involved in multiple phases of nitrate uptake.” *Plant Cell* 11: 865–874. https://doi.org/10.1105/tpc.11.5.865.

Liu, K. H., Y. Niu, M. Konishi, et al. 2017. “Discovery of nitrate–CPK–NLP signalling in central nutrient–growth networks.” *Nature* 545: 311–316. https://doi.org/10.1038/nature22077.

Liu, K. H., M. Liu, Z. Lin, et al. 2022. “NIN-like protein 7 transcription factor is a plant nitrate sensor.” *Science* 377: 1419–1425. https://doi.org/10.1126/science.add1104.

772 Maeda, Y., M. Konishi, T. Kiba, et al. 2018. "A NIGT1-centred transcriptional cascade regulates
773 nitrate signalling and incorporates phosphorus starvation signals in *Arabidopsis*." *Nature*
774 *Communications* 9: 1376. https://doi.org/10.1038/s41467-018-03832-6.
775
776 Marchive, C., F. Roudier, L. Castaings, et al. 2013. "Nuclear retention of the transcription factor
777 NLP7 orchestrates the early response to nitrate in plants." *Nature communications* 4: 1713.
778 https://doi.org/10.1038/ncomms2650.
779
780 Medici, A., and G. Krouk. 2014. "The primary nitrate response: a multifaceted signalling
781 pathway." *Journal of Experimental Botany* 65: 5567–5576. https://doi.org/10.1093/jxb/eru245.
782
783 Miyawaki, K., M. Matsumoto-Kitano, and T. Kakimoto. 2004. "Expression of cytokinin
784 biosynthetic isopentenyltransferase genes in *Arabidopsis*: tissue specificity and regulation by
785 auxin, cytokinin, and nitrate." *Plant Journal* 37: 128–138. https://doi.org/10.1046/j.1365-
786 313X.2003.01945.x.
787
788 Miyawaki, K., P. Tarkowski , M. Matsumoto-Kitano, et al. 2006. "Roles of *Arabidopsis*
789 ATP/ADP isopentenyltransferases and tRNA isopentenyltransferases in cytokinin biosynthesis."
790 *Proceedings of the National Academy of Sciences of the United States of America* 103: 16598–
791 16603. https://doi.org/10.1073/pnas.0603522103.
792
793 Monden, K., T. Kamiya, D. Sugiura, T. Suzuki, T. Nakagawa, and T. Hachiya. 2022. "Root-
794 specific activation of plasma membrane H^+-ATPase 1 enhances plant growth and shoot
795 accumulation of nutrient elements under nutrient-poor conditions in *Arabidopsis thaliana*."
796 *Biochemical and Biophysical Research Communications* 621: 39–45.
797 https://doi.org/10.1016/j.bbrc.2022.06.097.

Nacry, P., E. Bouguyon, and A. Gojon. 2013. “Nitrogen acquisition by roots: physiological and developmental mechanisms ensuring plant adaptation to a fluctuating resource.” *Plant and Soil* 370: 1–29. https://doi.org/10.1007/s11104-013-1645-9.

Ohkubo, Y., M. Tanaka, R. Tabata, M. Ogawa-Ohnishi, and Y. Matsubayashi. 2017. “Shoot-to-root mobile polypeptides involved in systemic regulation of nitrogen acquisition.” *Nature Plants* 3: 17029. https://doi.org/10.1038/nplants.2017.29.

Okamoto, Y., T. Suzuki, D. Sugiura, T. Kiba, H. Sakakibara, and T. Hachiya. 2019. “Shoot nitrate underlies a perception of nitrogen satiety to trigger local and systemic signaling cascades in *Arabidopsis thaliana*.” *Soil Science and Plant Nutrition* 65: 56–64. https://doi.org/10.1080/00380768.2018.1537643.

Osugi, A., M. Kojima, Y. Takebayashi, N. Ueda, T. Kiba, and H. Sakakibara. 2017. “Systemic transport of *trans*-zeatin and its precursor have differing roles in *Arabidopsis* shoots.” *Nature Plants* 3: 17112. https://doi.org/10.1038/nplants.2017.112.

Ota, R., Y. Ohkubo, Y. Yamashita, M. Ogawa-Ohnishi, and Y. Matsubayashi. 2020. “Shoot-to-root mobile CEPD-like 2 integrates shoot nitrogen status to systemically regulate nitrate uptake in *Arabidopsis*.” *Nature Communications* 11: 641. https://doi.org/10.1038/s41467-020-14440-8.

Patterson, K., L. A. Walters, A. M. Cooper, et al. 2016. “Nitrate-regulated glutaredoxins control Arabidopsis primary root growth.” *Plant Physiology* 170: 989–999. https://doi.org/10.1104/pp.15.01776.

824 Poitout, A., A. Crabos, I. Petřík, et al. 2018. “Responses to systemic nitrogen signaling in
825 Arabidopsis roots involve *trans*-zeatin in shoots.” *Plant Cell* 30: 1243–1257.
826 https://doi.org/10.1105/tpc.18.00011.
827
828 Rashotte, A. M., L. R. Goertzen. 2010. “The CRF domain defines cytokinin response factor
829 proteins in plants.” *BMC Plant Biology* 10: 74. https://doi.org/10.1186/1471-2229-10-74.
830
831 Remans, T., P. Nacry, M. Pervent, et al. 2006. “The *Arabidopsis* NRT1.1 transporter participates
832 in the signaling pathway triggering root colonization of nitrate-rich patches.” *Proceedings of the*
833 *National Academy of Sciences of the United States of America* 103: 19206–19211.
834 https://doi.org/10.1073/pnas.060527510.
835
836 Riveras, E., J. M. Alvarez, E. A. Vidal, C. Oses, A. Vega, and R. A. Gutiérrez. 2015. “The calcium
837 ion is a second messenger in the nitrate signaling pathway of Arabidopsis.” *Plant Physiology* 169:
838 1397–1404. https://doi.org/10.1104/pp.15.00961.
839
840 Rubin, G., T. Tohge, F. Matsuda, K. Saito, and W. R. Scheible. 2009. “Members of the *LBD*
841 family of transcription factors repress anthocyanin synthesis and affect additional nitrogen
842 responses in *Arabidopsis*.” *Plant Cell* 21: 3567–3584. https://doi.org/10.1105/tpc.109.067041.
843
844 Ruffel, S., G. Krouk, D. Ristova, D. Shasha, K. D. Birnbaum, and G. M. Coruzzi. 2011. “Nitrogen
845 economics of root foraging: transitive closure of the nitrate–cytokinin relay and distinct systemic
846 signaling for N supply vs. demand.” *Proceedings of the National Academy of Sciences of the*
847 *United States of America* 108: 18524–18529. https://doi.org/10.1073/pnas.1108684108.
848

849 Sakakibara, H., K. Takei, and N. Hirose. 2006. “Interactions between nitrogen and cytokinin in
850 the regulation of metabolism and development.” *Trends in Plant Science* 11: 440–448.
851 https://doi.org/10.1016/j.tplants.2006.07.004.
852
853 Sakakibara, H. 2021. “Cytokinin biosynthesis and transport for systemic nitrogen signaling.”
854 *Plant Journal* 105: 421–430. https://doi.org/10.1111/tpj.15011.
855
856 Safi, A., A. Medici, W. Szponarski, et al. 2021. “GARP transcription factors repress Arabidopsis
857 nitrogen starvation response via ROS-dependent and -independent pathways.” *Journal of*
858 *Experimental Botany* 72: 3881–3901. https://doi.org/10.1093/jxb/erab114.
859
860 Scheible, W. R., M. Lauerer, E. D. Schulze, M. Caboche, and M. Stitt. 1997. “Accumulation of
861 nitrate in the shoot acts as a signal to regulate shoot-root allocation in tobacco.” *Plant Journal* 11:
862 671–691. https://doi.org/10.1046/j.1365-313X.1997.11040671.x.
863
864 Signora, L., I. De Smet, C. H. Foyer, and H. Zhang. 2001. “ABA plays a central role in mediating
865 the regulatory effects of nitrate on root branching in *Arabidopsis*.” *Plant Journal* 28: 655–662.
866 https://doi.org/10.1046/j.1365-313x.2001.01185.x.
867
868 Su, H., T. Wang, C. Ju, et al. 2021. “Abscisic acid signaling negatively regulates nitrate uptake
869 via phosphorylation of NRT1. 1 by SnRK2s in *Arabidopsis*.” *Journal of Integrative Plant Biology*
870 63: 597–610. https://doi.org/10.1111/jipb.13057.
871
872 Tabata, R., K. Sumida, T. Yoshii, K. Ohyama, H. Shinohara, and Y. Matsubayashi. 2014.
873 “Perception of root-derived peptides by shoot LRR-RKs mediates systemic N-demand signaling.”
874 *Science* 346: 343–346. DOI: 10.1126/science.1257800.

875

876 Takei, K., N. Ueda, K. Aoki, et al. 2004a. "*AtIPT3* is a key determinant of nitrate-dependent
877 cytokinin biosynthesis in *Arabidopsis*." *Plant & Cell Physiology* 45: 1053–1062.
878 https://doi.org/10.1093/pcp/pch119.

879

880 Takei, K., T. Yamaya, and H. Sakakibara. 2004b. "Arabidopsis *CYP735A1* and *CYP735A2*
881 encode cytokinin hydroxylases that catalyze the biosynthesis of *trans*-zeatin." *Journal of*
882 *Biological Chemistry* 279: 41866–41872. https://doi.org/10.1074/jbc.M406337200.

883

884 Tokunaga, H., M. Kojima, T. Kuroha, et al. 2011. "Arabidopsis lonely guy (LOG) multiple
885 mutants reveal a central role of the LOG-dependent pathway in cytokinin activation." *Plant*
886 *Journal* 69: 355–365. https://doi.org/10.1111/j.1365-313X.2011.04795.x.

887

888 Wang, R., R. Tischner, R. A. Gutiérrez, et al. 2004. "Genomic analysis of the nitrate response
889 using a nitrate reductase-null mutant of Arabidopsis." *Plant Physiology* 136: 2512–2522.
890 https://doi.org/10.1104/pp.104.044610.

891

892 Wang, R, X. Xing, and N. M. Crawford. 2007. "Nitrite acts as a transcriptome signal at
893 micromolar concentrations in Arabidopsis roots." *Plant Physiology* 145: 1735–1745.
894 https://doi.org/10.1104/pp.107.108944.

895

896 Wang, X., C. Feng, L. Tian, et al. 2021. "A transceptor–channel complex couples nitrate sensing
897 to calcium signaling in *Arabidopsis*." *Molecular Plant* 14: 774–786.
898 https://doi.org/10.1016/j.molp.2021.02.005.

899

900 Werner, T., V. Motyka, V. Laucou, R. Smets, H. Van Onckelen, and T. Schmülling. 2003.
901 "Cytokinin-deficient transgenic Arabidopsis plants show multiple developmental alterations
902 indicating opposite functions of cytokinins in the regulation of shoot and root meristem activity."
903 *Plant Cell* 15: 2532–2550. https://doi.org/10.1105/tpc.014928.
904
905 Werner, T., K. Holst, Y. Pörs, et al. 2008. "Cytokinin deficiency causes distinct changes of sink
906 and source parameters in tobacco shoots and roots." *Journal of Experimental Botany* 59: 2659–
907 2672. https://doi.org/10.1093/jxb/ern134.
908
909 Werner, T., Schmülling, T. 2009. "Cytokinin action in plant development." *Current Opinion in*
910 *Plant Biology* 12: 527–538. https://doi.org/10.1016/j.pbi.2009.07.002.
911
912 Wu, B., J. Meng, H. Liu, et al. 2023. "Suppressing a phosphohydrolase of cytokinin nucleotide
913 enhances grain yield in rice." *Nature Genetics* 55: 1381–1389. https://doi.org/10.1038/s41588-
914 023-01454-3.
915
916 Xu, N., R. Wang, L. Zhao, et al. 2016. "The Arabidopsis NRG2 protein mediates nitrate signaling
917 and interacts with and regulates key nitrate regulators." *Plant Cell* 28: 485–504.
918 https://doi.org/10.1105/tpc.15.00567.
919
920 Zhou, Y., B. Zhou, L. Pache, et al. 2019. "Metascape provides a biologist-oriented resource for
921 the analysis of systems-level datasets." *Nature Communications* 10: 1523.
922 https://doi.org/10.1038/s41467-019-09234-6.
923

924 Zhang, H., A. Jennings, P. W. Barlow, and B. G. Forde. 1999. "Dual pathways for regulation of
925 root branching by nitrate." *Proceedings of the National Academy of Sciences of the United States*
926 *of America* 96: 6529–6534. https://doi.org/10.1073/pnas.96.11.6529.
927

928 **Supporting Information**

929 Additional supporting information can be found online in the Supporting Information section.

930

931 **Figure Legends**

932 **Figure 1.** Micrografting and transfer experiments for manipulation of nitrate levels and *IPT3*
933 expression in a shoot-specific manner. (A) Summary of the micrografting and transfer
934 experiments. (B) A schematic representation of four types of grafted plants. The dotted line
935 represents the grafted seam in the hypocotyl. (C, D) Nitrate concentrations in shoots (C) and roots
936 (D) 0, 3, or 5 days after nitrogen removal. (E, F) Total protein concentrations in shoots (E) and
937 roots (F) 5 days after nitrogen removal. (C–F) Two grafted plants were pooled as one biological
938 replicate. Data are presented as mean ± SD (n = 3). (G, H) Total nitrogen concentrations in shoots
939 (G) and roots (H) 5 days after nitrogen removal. Sampling was performed three times
940 independently. In this sampling, 7, 6, and 5 grafted plants were pooled as one biological replicate.
941 Data are presented as mean ± SD (n = 3). (C–H) Different lowercase letters indicate significant
942 differences, as determined via Tukey–Kramer test ($P < 0.05$). (I) Transcript levels of *IPT3* in
943 shoots 5 days after nitrogen removal, as determined using RT-qPCR. Sampling was done five
944 times independently. In this sampling, 9, 6, 7, 7, and 8 grafted plants were pooled as one biological
945 replicate. Data are presented as mean ± SD (n = 5). (J) Nitrate concentrations in shoots 5 days
946 after nitrogen removal. (K) Transcript levels of *GFP* in shoots 5 days after nitrogen removal, as
947 determined via RT-qPCR. (J, K) One biological replicate consisted of one grafted plant. Data are
948 presented as mean ± SD (n = 3). (I–K) Statistical significance was assessed using unpaired two-
949 tailed Welch's *t*-test (*$P < 0.05$; **$P < 0.01$; ***$P < 0.001$). (L) Fluorescence images of true

950 leaves 5 days after nitrogen removal. Green and red colors correspond to GFP fluorescence and
951 autofluorescence, respectively. Scale bars represent 500 μm. In graph legends, the grafted plants
952 are indicated as "scion line name/rootstock line name." ns, not significant; FW, fresh weight; DW,
953 dry weight.
954
955 **Figure 2.** Effects of shoot nitrate status and shoot *IPT3* expression on the shoot and root
956 concentrations of CK species. (A–M) The shoot and root concentrations of iP (A), iPR (B), iPRPs
957 (C), iP7G (D), iP9G (E), *t*Z (F), *t*ZR (G), *t*ZPRs (H), *t*Z7G (I), *t*Z9G (J), *t*ZOG (K), *t*ZROG (L),
958 and *t*ZRPsOG (M) in the grafted plants 5 days after nitrogen removal (condition 5). Sampling
959 was performed three times independently. In the sampling, 7, 6, and 5 grafted plants were pooled
960 as one biological replicate. Data are presented as mean ± SD [n = 3, excluding iP concentrations
961 in Col/*ipt3,5,7* roots and *ipt3*/*ipt3,5,7* roots (n = 2)]. Different lowercase letters indicate
962 significant differences, as determined via Tukey–Kramer test ($P < 0.05$). iP, N^6-(Δ^2-
963 isopentenyl)adenine; iPR, iP riboside; iPRPs, iP ribotides; iP7G, iP-7-*N*-glucoside; iP9G, iP-9-*N*-
964 glucoside; *t*Z, *trans*-zeatin; *t*ZR, *t*Z riboside; *t*ZRPs, *t*Z ribotides; *t*Z7G, *t*Z-7-*N*-glucoside; *t*Z9G,
965 *t*Z-9-*N*-glucoside; *t*ZOG, *t*Z-*O*-glucoside; *t*ZROG, *t*ZR-*O*-glucoside; *t*ZRPsOG, *t*ZRPs-*O*-
966 glucoside; ns, not significant; nd, not detected; FW, fresh weight.
967
968 **Figure 3.** Effects of shoot nitrate status and shoot *IPT3* expression on plant growth. (A)
969 Representative shoot appearance of grafted plants. Scale bars represent 5 mm. (B–F) Shoot fresh
970 weight (B), leaf blade area (C), rosette diameter (D), leaf number (E), root fresh weights (F), and
971 fresh weight ratios of shoot to root (G) of grafted plants 5 days after nitrogen removal (condition
972 5). All data pooled from five independent grafting experiments are presented as mean ± SD (n =
973 33). Different lowercase letters indicate significant differences, as determined via Tukey–Kramer
974 test ($P < 0.05$). ns, not significant; FW, fresh weight.

975

976 **Figure 4.** Effects of shoot nitrate status and shoot *IPT3* expression on the shoot and root
977 transcriptomes. RNA-seq was performed using the shoots and roots of grafted plants 5 days after
978 nitrogen removal (condition 5). Sampling was performed three times independently. In the
979 sampling, 9, 6, and 7 grafted plants were pooled as one biological replicate. (A) Venn diagram
980 presenting the number of DEGs at a minimum fold change of 1.5 in NR-null/*ipt3,5,7* plants
981 relative to Col/*ipt3,5,7* plants and in NR-null *ipt3*/*ipt3,5,7* plants relative to *ipt3*/*ipt3,5,7* plants.
982 Statistical significance of overlap was assessed using the hypergeometric test (*$P < 0.05$;
983 **$P < 0.01$; ***$P < 0.001$). (B–E) Plots of normalized transcript levels of 631 DEGs (B) and 663
984 DEGs (C) in shoots and 189 DEGs (D) and 126 DEGs (E) in roots. 1st, 2nd, and 3rd denote the
985 order of three independent experiments. Different lowercase letters indicate significant
986 differences, as determined via Tukey–Kramer test ($P < 0.05$). The numbers on the graph represent
987 the difference in mean values.

988

989 **Figure 5.** Effects of shoot nitrate status and shoot *IPT3* expression on nitrogen-related
990 transcriptional responses in shoots and roots. (A–D) Plots of mean normalized transcript levels of
991 nitrate (*per se*)-inducible genes in 2 h (A), genes induced via CPK10/30/32 (B), genes commonly
992 induced via all NLPs (C), and nitrogen starvation-inducible genes (D) in the shoots and roots of
993 grafted plants 5 days after nitrogen removal (condition 5). The gene lists were obtained from
994 Wang et al. (2004) for (A), Liu et al. (2017) for (B), Liu et al. (2022) for (C), and Kiba et al.
995 (2018) and Krapp et al. (2011) for (D). The numbers on the graph represent the difference in mean
996 values. (E–H) Transcriptional changes in genes involved in nitrogen transport and assimilation in
997 roots (E), genes encoding transcription factors for nitrogen starvation responses in shoots (F) and
998 in roots (G), and genes encoding shoot-to-root mobile peptides in shoots (H) in grafted plants 5
999 days after nitrogen removal. The normalized transcript levels were visualized as heatmaps using
1000 MORPHEUS (https://software.broadinstitute.org/morpheus). The relative color scheme uses the

1001 minimum (blue) and maximum (yellow) values in each row. 1st, 2nd, and 3rd denote the order of
1002 three independent experiments. TF, transcription factor. (A–H) Different lowercase letters
1003 indicate significant differences, as determined via Tukey–Kramer test ($P < 0.05$). ns, not
1004 significant.
1005
1006 **Figure 6.** Summary of systemic responses to shoot nitrate accumulation and their dependence by
1007 shoot IPT3.

Figure 1

(A) Procedure for transfer experiment

	Condition 1 →	Condition 2 →	Condition 3 →	Condition 4 →	Condition 5
Duration	4 days	5 days	24 hours	24 hours	0, 3, 5 days
N source	2.5 mM NH_4^+	2.5 mM NH_4^+	2.5 mM NH_4^+	10 mM NO_3^- & 2.5 mM NH_4^+	No nitrogen
pH	6.7	6.7	6.7	6.7	5.7
PPFD	25 μmol m^{-2} s^{-1}	50 μmol m^{-2} s^{-1}	25 μmol m^{-2} s^{-1}	25 μmol m^{-2} s^{-1}	25 μmol m^{-2} s^{-1}
Temperature	22°C	27°C	22°C	22°C	22°C

▲ Micrografting ▲ NO_3^- supply ▲ Nitrogen removal

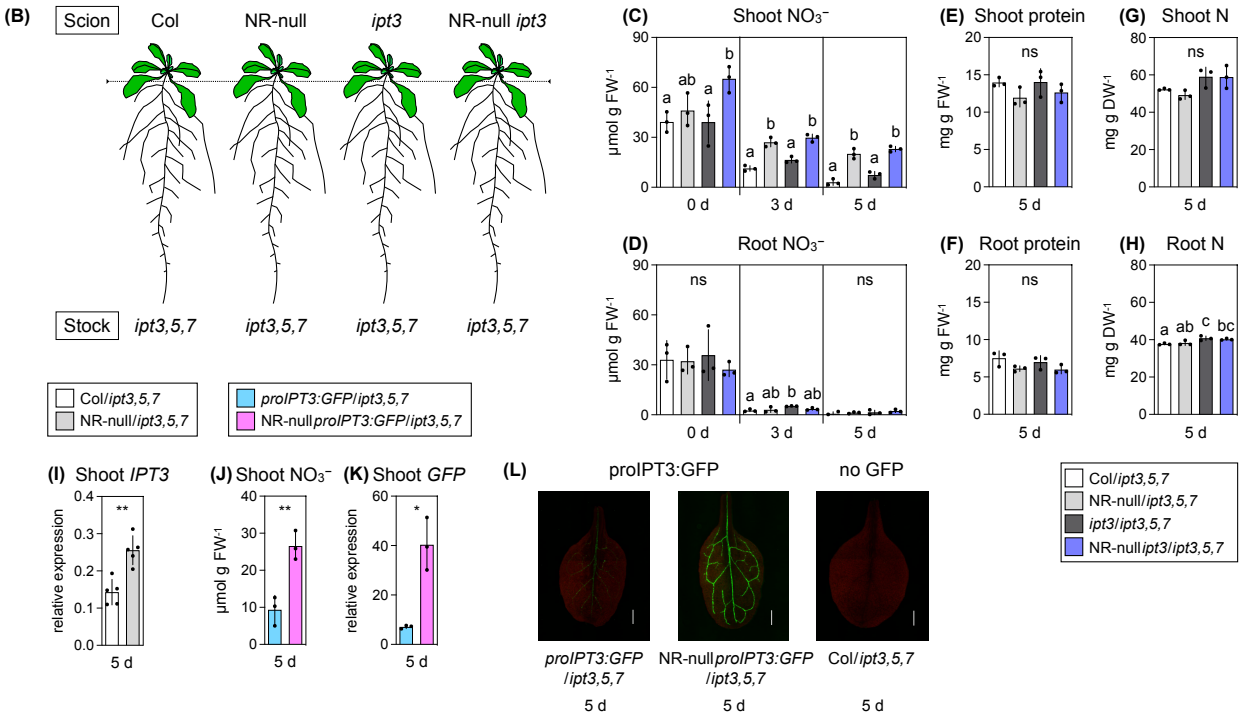

Figure 1. Micrografting and transfer experiments for manipulation of nitrate levels and *IPT3* expression in a shoot-specific manner. (A) Summary of the micrografting and transfer experiments. (B) A schematic representation of four types of grafted plants. The dotted line represents the grafted seam in the hypocotyl. (C, D) Nitrate concentrations in shoots (C) and roots (D) 0, 3, or 5 days after nitrogen removal. (E, F) Total protein concentrations in shoots (E) and roots (F) 5 days after nitrogen removal. (C–F) Two grafted plants were pooled as one biological replicate. Data are presented as mean ± SD (n = 3). (G, H) Total nitrogen concentrations in shoots (G) and roots (H) 5 days after nitrogen removal. Sampling was performed three times independently. In this sampling, 7, 6, and 5 grafted plants were pooled as one biological replicate. Data are presented as mean ± SD (n = 3). (C–H) Different lowercase letters indicate significant differences, as determined via Tukey–Kramer test ($P < 0.05$). (I) Transcript levels of *IPT3* in shoots 5 days after nitrogen removal, as determined using RT-qPCR. Sampling was done five times independently. In this sampling, 9, 6, 7, 7, and 8 grafted plants were pooled as one biological replicate. Data are presented as mean ± SD (n = 5). (J) Nitrate concentrations in shoots 5 days after nitrogen removal. (K) Transcript levels of *GFP* in shoots 5 days after nitrogen removal, as determined via RT-qPCR. (J, K) One biological replicate consisted of one grafted plant. Data are presented as mean ± SD (n = 3). (I–K) Statistical significance was assessed using unpaired two-tailed Welch's *t*-test (*$P < 0.05$; **$P < 0.01$; ***$P < 0.001$). (L) Fluorescence images of true leaves 5 days after nitrogen removal. Green and red colors correspond to GFP fluorescence and autofluorescence, respectively. Scale bars represent 500 μm. In graph legends, the grafted plants are indicated as "scion line name/rootstock line name." ns, not significant; FW, fresh weight; DW, dry weight.

Figure 2

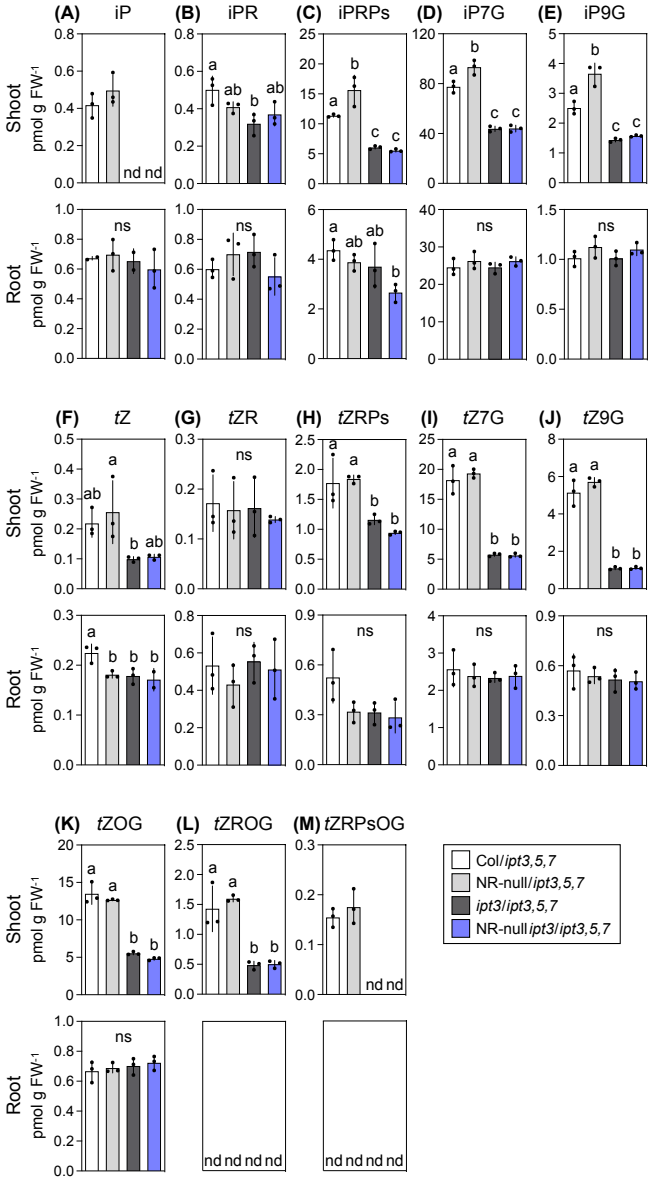

Figure 2. Effects of the shoot nitrate status and shoot *IPT3* expression on the shoot and root concentrations of CK species. (A–M) The shoot and root concentrations of iP (A), iPR (B), iPRPs (C), iP7G (D), iP9G (E), *t*Z (F), *t*ZR (G), *t*ZPRs (H), *t*Z7G (I), *t*Z9G (J), *t*ZOG (K), *t*ZROG (L), and *t*ZRPsOG (M) in the grafted plants 5 days after nitrogen removal (condition 5). Sampling was performed three times independently. In the sampling, 7, 6, and 5 grafted plants were pooled as one biological replicate. Data are presented as mean ± SD [n = 3, excluding iP concentrations in Col/*ipt3,5,7* roots and *ipt3*/*ipt3,5,7* roots (n = 2)]. Different lowercase letters indicate significant differences, as determined via Tukey–Kramer test ($P < 0.05$). iP, N^6-(Δ^2-isopentenyl)adenine; iPR, iP riboside; iPRPs, iP ribotides; iP7G, iP-7-*N*-glucoside; iP9G, iP-9-*N*-glucoside; *t*Z, *trans*-zeatin; *t*ZR, *t*Z riboside; *t*ZRPs, *t*Z ribotides; *t*Z7G, *t*Z-7-*N*-glucoside; *t*Z9G, *t*Z-9-*N*-glucoside; *t*ZOG, *t*Z-*O*-glucoside; *t*ZROG, *t*ZR-*O*-glucoside; *t*ZRPsOG, *t*ZRPs-*O*-glucoside; nd, not detected; FW, fresh weight.

Figure 3

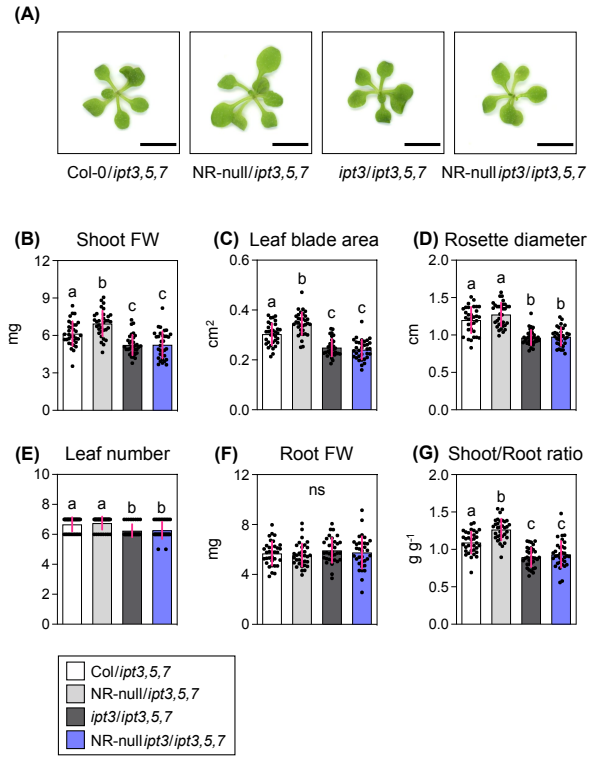

Figure 3. Effects of the shoot nitrate status and shoot *IPT3* expression on plant growth. (A) Representative shoot appearance of grafted plants. Scale bars represent 5 mm. (B–F) Shoot fresh weights (B), leaf blade area (C), rosette diameter (D), leaf number (E), root fresh weights (F), and fresh weight ratios of shoot to root (G) of grafted plants 5 days after nitrogen removal (condition 5). All data pooled from five independent grafting experiments are presented as mean ± SD (n = 33). Different lowercase letters indicate significant differences, as determined via Tukey–Kramer test ($P < 0.05$). ns, not significant; FW, fresh weight.

Figure 4

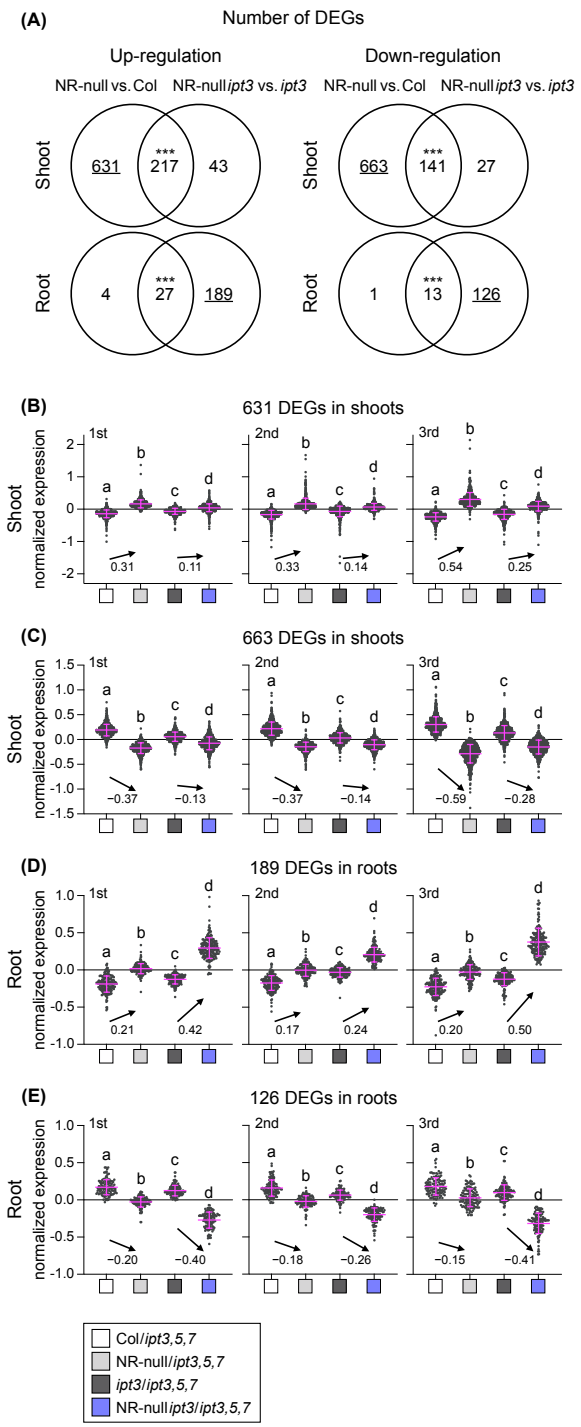

Figure 4. Effects of the shoot nitrate status and shoot *IPT3* expression on the shoot and root transcriptomes. RNA-seq was performed using the shoots and roots of grafted plants 5 days after nitrogen removal (condition 5). Sampling was performed three times independently. In the sampling, 9, 6, and 7 grafted plants were pooled as one biological replicate. (A) Venn diagram presenting the number of DEGs at a minimum fold change of 1.5 in NR-null/*ipt3,5,7* plants relative to Col/*ipt3,5,7* plants and in NR-null *ipt3*/*ipt3,5,7* plants relative to *ipt3*/*ipt3,5,7* plants. Statistical significance of overlap was assessed using the hypergeometric test (*$P < 0.05$; **$P < 0.01$; ***$P < 0.001$). (B–E) Plots of normalized transcript levels of 631 DEGs (B) and 663 DEGs (C) in shoots and 189 DEGs (D) and 126 DEGs (E) in roots. 1st, 2nd, and 3rd denote the order of three independent experiments. Different lowercase letters indicate significant differences, as determined via Tukey–Kramer test ($P < 0.05$). The numbers on the graph represent the difference in mean values.

Figure 5

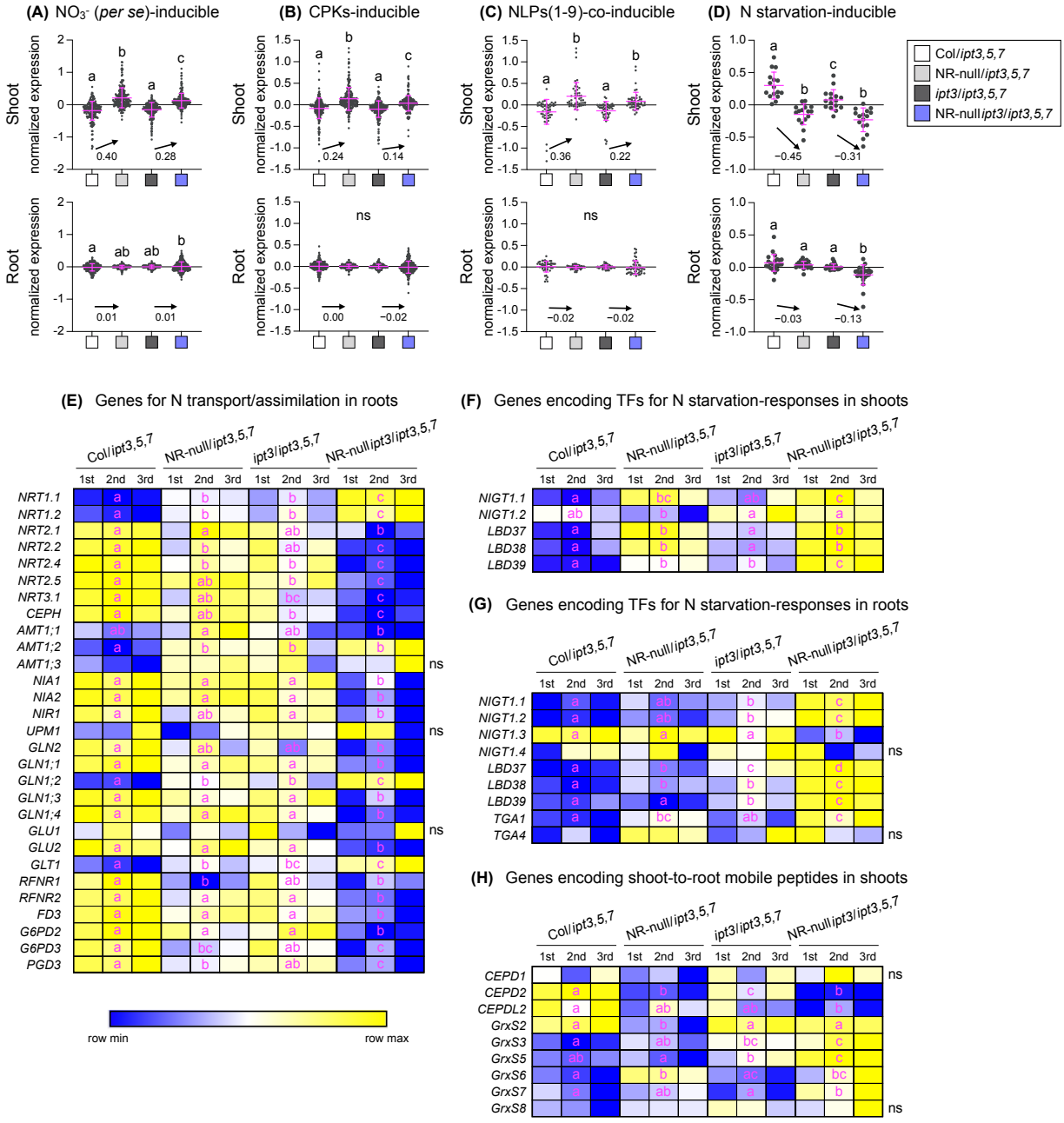

Figure 5. Effects of the shoot nitrate status and shoot *IPT3* expression on nitrogen-related transcriptional responses in shoots and roots. (A–D) Plots of mean normalized transcript levels of nitrate (*per se*)-inducible genes in 2 h (A), genes induced via CPK10/30/32 (B), genes commonly induced via all NLPs (C), and nitrogen starvation-inducible genes (D) in the shoots and roots of grafted plants 5 days after nitrogen removal (condition 5). The gene lists were obtained from Wang et al. (2004) for (A), Liu et al. (2017) for (B), Liu et al. (2022) for (C), and Kiba et al. (2018) and Krapp et al. (2011) for (D). The numbers on the graph represent the difference in mean values. (E–H) Transcriptional changes in genes involved in nitrogen transport and assimilation in roots (E), genes encoding transcription factors for nitrogen starvation responses in shoots (F) and in roots (G), and genes encoding shoot-to-root mobile peptides in shoots (H) in grafted plants 5 days after nitrogen removal. The normalized transcript levels were visualized as heatmaps using MORPHEUS (https://software.broadinstitute.org/morpheus). The relative color scheme uses the minimum (blue) and maximum (yellow) values in each row. 1st, 2nd, and 3rd denote the order of three independent experiments. TF, transcription factor. (A–H) Different lowercase letters indicate significant differences, as determined via Tukey–Kramer test ($P < 0.05$). ns, not significant;

Figure 6

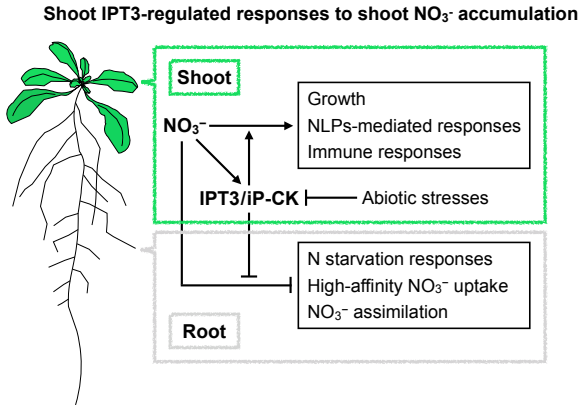

Figure 6. Summary of systemic responses to shoot nitrate accumulation and their modulation by shoot IPT3.